

**DETECTION OF SCOUR DEPTH USING SINGLEMODE-
MULTIMODE-SINGLEMODE FIBER SENSOR**

NORSHAZMIRA BINTI MAT AZMI

**FACULTY OF ENGINEERING
UNIVERSITY OF MALAYA
KUALA LUMPUR**

2018

**DETECTION OF SCOUR DEPTH USING
SINGLEMODE-MULTIMODE-SINGLEMODE FIBER
SENSOR**

NORSHAZMIRA BIBTI MAT AZMI

**DISSERTATION SUBMITTED IN FULFILMENT OF
THE REQUIREMENTS FOR THE DEGREE OF MASTER
OF ENGINEERING SCIENCE**

**FACULTY OF ENGINEERING
UNIVERSITY OF MALAYA
KUALA LUMPUR**

2018

UNIVERSITY OF MALAYA
ORIGINAL LITERARY WORK DECLARATION

Name of Candidate: NORSHAZMIRA MAT AZMI

I.C/Passport No:

Matric No: KGA140074

Name of Degree: MASTER OF ENGINEERING SCIENCE

Title of Project Paper/Research Report/Dissertation/Thesis (“this Work”):

DETECTION OF SCOUR DEPTH USING SINGLEMODE-MULTIMODE-
SINGLEMODE FIBER SENSOR

Field of Study:

CIVIL ENGINEERING

I do solemnly and sincerely declare that:

- (1) I am the sole author/writer of this Work;
- (2) This Work is original;
- (3) Any use of any work in which copyright exists was done by way of fair dealing and for permitted purposes and any excerpt or extract from, or reference to or reproduction of any copyright work has been disclosed expressly and sufficiently and the title of the Work and its authorship have been acknowledged in this Work;
- (4) I do not have any actual knowledge nor do I ought reasonably to know that the making of this work constitutes an infringement of any copyright work;
- (5) I hereby assign all and every rights in the copyright to this Work to the University of Malaya (“UM”), who henceforth shall be owner of the copyright in this Work and that any reproduction or use in any form or by any means whatsoever is prohibited without the written consent of UM having been first had and obtained;
- (6) I am fully aware that if in the course of making this Work I have infringed any copyright whether intentionally or otherwise, I may be subject to legal action or any other action as may be determined by UM.

Candidate’s Signature

Date:

Subscribed and solemnly declared before,

Witness’s Signature

Date:

Name:

Designation:

DETECTION OF SCOUR DEPTH USING SINGLEMODE-MULTIMODE- SINGLEMODE FIBER SENSOR

ABSTRACT

This thesis presents an experimental study in the laboratory to develop and test a method for continuously measuring and monitoring scour using Single mode-Multimode-Singlemode (SMS) sensor. The study provides an insight into the SMS technology and develops the framework using this technology to eventually address central theme in river mechanics and sediment transport; which is the scour/deposition depth around a hydraulic structure. In particular, this study develops a new packaging method for the sensor to detect the extent of local scour where a set of experiments are performed using hydraulic flume for a duration of 900 minutes with a maximum scour depth of 27 mm. The experiments presented herein are classified into two main groups, (1) the laboratory work to develop the sensor package and (2) the wavelength shift vs. the scour depth experiments. The laboratory results show that the sensor has a potential to be applied in a real-time monitoring application such as in bridge scouring. Wavelength shifts of 0.12 nm and 0.06 nm are observed at the transitions between different phases in the development of local scour around PVC pipe.

Keywords: SMS sensor, scour, hydraulic, experiments

DETECTION OF SCOUR DEPTH USING SINGLEMODE-MULTIMODE- SINGLEMODE FIBER SENSOR

ABSTRAK

Tesis ini membentangkan satu kajian eksperimen di makmal untuk membangunkan dan menguji kaedah untuk mengukur dan memantau hakisan secara berterusan menggunakan sensor Singlemode-Multimode-Singlemode (SMS). Kajian ini memberi kefahaman tentang teknologi SMS dan membangunkan rangka kerja bagi menggunakan teknologi ini untuk akhirnya menangani isu utama mekanik sungai dan pengangkutan sedimen; iaitu kedalaman hakisan / pemendapan di sekitar struktur hidraulik. Kajian ini membangunkan kaedah pakej baru bagi sensor untuk mengesan sejauh mana hakisan tempatan (local scour) di mana satu set eksperimen yang dilakukan dengan menggunakan flum hidraulik untuk tempoh 900 minit dengan kedalaman hakisan maksimum 27 mm. Eksperimen yang dibentangkan ini dikelaskan kepada dua kumpulan utama: (1) kerja-kerja makmal untuk membangunkan pakej sensor dan (2) eksperimen perubahan gelombang sensor melawan kedalaman hakisan. Keputusan makmal menunjukkan bahawa sensor ini berpotensi untuk diaplikasikan sebagai sensor pemantauan hakisan di kawasan jambatan. Perubahan pada gelombang sensor 0.12 nm dan 0.06nm diperhatikan pada peralihan antara fasa yang berbeza dalam pembentukan hakisan tempatan (local scour) di sekeliling paip PVC.

Keywords: SMS sensor, scour, hidraulik, experiments

ACKNOWLEDGEMENTS

After ALLAH swt, I would like to express my deepest gratitude to my supervisor, Prof. Dr. Sulaiman Wadi Harun, co-supervisor, Dr. Mohamed Jameel, and Assoc. Prof. Dr. Shatirah as my external supervisor for their invaluable kindness, patience, advice, and support. They showed themselves to me as a model scientists and teachers that I eagerly wish to follow. This work would never have been completed without their support and assistance. A special thanks and appreciation go to all the academic staff and the laboratory assistants at Civil Engineering Department, University of Malaya.

I gratefully acknowledged my colleagues, Dr. Zarif and Sayidal El Fatimah and Khairunisa Md Nasir who have helped me a lot in the experimental, especially with the practical issue of SMS fabrications, installations and applications.

I would like to acknowledge the grant (HIR Grant) provided from University of Malaya to fulfill the research works.

Special thanks go to my parents, Mat Azmi Bin Jusoh and Faridah Binti Jaapar also to my brothers for their continuous support, prayer, and patience throughout the years.

TABLE OF CONTENTS

| | |
|--|-----------|
| ABSTRACT | 1 |
| ABSTRAK..... | 2 |
| ACKNOWLEDGEMENTS | 3 |
| TABLE OF CONTENTS..... | 4 |
| LIST OF FIGURES..... | 6 |
| LIST OF TABLES..... | 8 |
| LIST OF SYMBOLS AND ABBREVIATIONS..... | 9 |
| CHAPTER 1: INTRODUCTION | 10 |
| 1.1. General Background..... | 10 |
| 1.2. Singlemode-Multimode-Singlemode Fiber (SMS) Structure | 13 |
| 1.3. Problem Statement | 14 |
| 1.4. Research Aim and Objectives | 14 |
| 1.5. Research Significance | 14 |
| 1.6. Organization of the Thesis | 15 |
| CHAPTER 2: LITERATURE REVIEW | 16 |
| 2.1. Bridge Problem in Malaysia..... | 16 |
| 2.2. Scour | 17 |
| 2.2.1. Factors that Influencing Scour | 20 |
| 2.2.2. Specific Parameter on Local Scour | 22 |
| 2.2.3. Effect of Flow Intensity, V/V_c | 24 |
| 2.2.4. Predicting Equilibrium Scour depth..... | 26 |
| 2.3. Scour Detection Device..... | 26 |
| 2.4. Singlemode-Multimode-Singlemode (SMS) Structure..... | 27 |
| 2.5. Summary | 29 |
| CHAPTER 3: MATERIALS AND METHODS..... | 30 |

| | |
|--|-----------|
| 3.1. Introduction | 30 |
| 3.2. Materials and Equipment | 30 |
| 3.2.1. Optical Fiber..... | 30 |
| 3.2.2. Fusion Splicer | 32 |
| 3.2.3. Optical Spectrum Analyzer | 33 |
| 3.2.4. Amplified Spontaneous Emission (ASE) Light Source | 34 |
| 3.2.5. Pier Model..... | 34 |
| 3.2.6. Coarse Sand..... | 35 |
| 3.2.7. Control Block | 36 |
| 3.2.8. Hydraulic Flume..... | 37 |
| 3.2.9. Water Condition | 39 |
| 3.3. Research Methodology..... | 40 |
| 3.3.1. Splicing Fiber | 40 |
| 3.3.2. Singlemode-Multimode-Singlemode (SMS) Sensor Package | 42 |
| 3.3.3. Sensor Installation and Experimental Setup | 44 |
| CHAPTER 4: RESULTS AND DISCUSSION..... | 48 |
| 4.1. Scouring Result | 48 |
| 4.2. Bandpass Filtering Characteristic of SMS Structure | 50 |
| 4.3. Scouring Depth and Wavelength Change | 51 |
| CHAPTER 5: CONCLUSION AND FUTURE WORK RECOMMENDATION | 57 |
| 5.1. Conclusion | 57 |
| 5.2. Recommendations for Further Investigation..... | 57 |
| REFERENCES | 59 |
| LIST OF PUBLICATIONS AND PAPERS PRESENTED..... | 63 |

LIST OF FIGURES

| | |
|--|----|
| Figure 1.1: The Willow Creek bridge failure, where the bed elevation was lowered due to erosion. (Ettema et al., 2006) | 11 |
| Figure 1.2: Skatch of bridge crossings | 11 |
| Figure 1.3: A bridge failure in Wild River, Minnesota case caused by the interrelated action of scour and debris accumulation against the structure. (Ettema et al., 2006) | 12 |
| Figure 2.1: General scouring of riverbed at Sg. Jeniang | 17 |
| Figure 2.2: Failure of Bulls Road Bridge, Rangitikei River, NZ, June 1973 (Melville & Coleman, 2000) | 19 |
| Figure 2.3: Scour at a cylindrical pier (Lagasse & Richardson, 2001) | 20 |
| Figure 2.4: Local scour depth variation with sediment coarseness (Melville & Coleman, 2000) | 23 |
| Figure 2.5: Local scour depth variation with sediment non-uniformity (Melville & Coleman, 2000) | 24 |
| Figure 2.6: Pier scour depth in a sand-bed (Lagasse & Richardson, 2001) | 25 |
| Figure 3.1: Optical fiber structure | 31 |
| Figure 3.2: Images of the commercial fibers used in the experiment (a) SMF (b) MMF. | 32 |
| Figure 3.3: Fujikura Arc Fusion Splicer (a) outside view (b) screen view | 33 |
| Figure 3.4: Anritsu Optical Spectrum Analyzer used in this work | 34 |
| Figure 3.5: Pier model made of PVC pipe | 35 |
| Figure 3.6: Coarse sand used in the experiments | 36 |
| Figure 3.7: Control block used during the hydraulic experiment | 37 |
| Figure 3.8: Hydraulic Flume | 38 |
| Figure 3.9: Opening Gauge of the flume | 38 |
| Figure 3.10: Graphic user interface of the InduSoft Software, which is used to control water flow into hydraulic flume | 39 |
| Figure 3.11: Steps of splicing fiber | 41 |

| | |
|---|----|
| Figure 3.12: Stages to package the SMS Sensor..... | 43 |
| Figure 3.13:SMS sensor package..... | 43 |
| Figure 3.14: Installation of the package SMS structure for local scour monitoring on a PVC pipe. | 45 |
| Figure 3.15: Photo images of (a) – (b) Sediment piling at the sensor and PVC assembly. (c) Process of leveling and distribution of sediment and (d) model in flume before experiment start..... | 46 |
| Figure 3.16: Images of the sensor probe during the experiment..... | 47 |
| Figure 4.1: Scour depth, d_s/B versus time scour occur at the PVC pipe | 50 |
| Figure 4.2: Bandpass filtering characteristic of the packaged SMS structure | 51 |
| Figure 4.3: Measured depth and scour depth at different time interval | 52 |
| Figure 4.4: Photo images of PVC pipe scouring at different period of 100 mins..... | 53 |
| Figure 4.5: Photo images of PVC pipe scouring at different period of 420 mins..... | 53 |
| Figure 4.6: Sensor bandpass filter interferometer spectra at different time interval..... | 55 |
| Figure 4.7: Dimensionless scour depth and dip center wavelength 1 curves for duration of 900 mins..... | 55 |
| Figure 4.8: Dimensionless scour depth and dip center wavelength 2 curves for duration of 900 mins..... | 56 |

LIST OF TABLES

Table 2.1: Classification of local scour process at bridge foundations.....23

Table 4.1: Result for experiment of scour using PVC pipe model. d_s is a scour depth, B is pier width and d_s/B is a dimensionless scour depth49

University of Malaya

LIST OF SYMBOLS AND ABBREVIATIONS

| | | |
|-----------|---|---------------------------------|
| SMF | : | Single Mode Fiber |
| MMF | : | Multi Mode Fiber |
| SMS | : | Singlemode-Multimode-Singlemode |
| FBG | : | Fiber Bragg Grating |
| PVC | : | Polyvinyl Chloride |
| d_0 | : | Depth Flow |
| d_s | : | Scour Depth |
| d_{50} | : | Median Sediment Size |
| y/B | : | flow shallowness |
| B | : | Pier width |
| V | : | Velocity |
| V_a | : | Mean Approach Velocity |
| V_c | : | Critical Velocity |
| ASE | : | Amplified Spontaneous Emission |
| OSA | : | Optical Spectrum Analyzer |
| Db | : | Decibel |
| λ | : | Wavelength |

CHAPTER 1: INTRODUCTION

1.1. General background

Scour is defined as the removal of channel bed sediments under the erosive action of the flow. Extreme scour will lead to exposing subsoil and can badly affect channel stability and laterally eroding the riverbanks (Ettema, Nakato, & Muste, 2006) (Figure 1.1). The instability of channel will increase the potential of the hydraulic structures that located in the channel to fail or collapse. It is challenging for a bridge designer to design a stable bridge foundation because bridges cannot adapt to a dynamically changing riverine environment. To efficiently accommodate the flow and sediment discharges, rivers gradually alter their banks and beds.

Moreover, the main channel at bridge crossings will cause increased turbulence and stream flow velocities below the bridge opening and lead to result excessive bridge scour (Figure 1.2). Afterwards, the bed sediments around bridge piers and abutments are washed away, compromising the bridge foundations. Scour around bridge foundations (e.g., piers and abutments) can lead to their failure during high floods (Figure 1.3). Bridge scour has been identified as a problem at a national scale, being both an economic burden and a threat to public safety. In recent history, more bridge failures have been attributed to scour than all other causes combined (King & Mahamud, 2009). Therefore, the scour measurement is becoming important to avoid any bridge failures.



Figure 1.1: The Willow Creek bridge failure, where the bed elevation was lowered due to erosion. (Ettema et al., 2006)

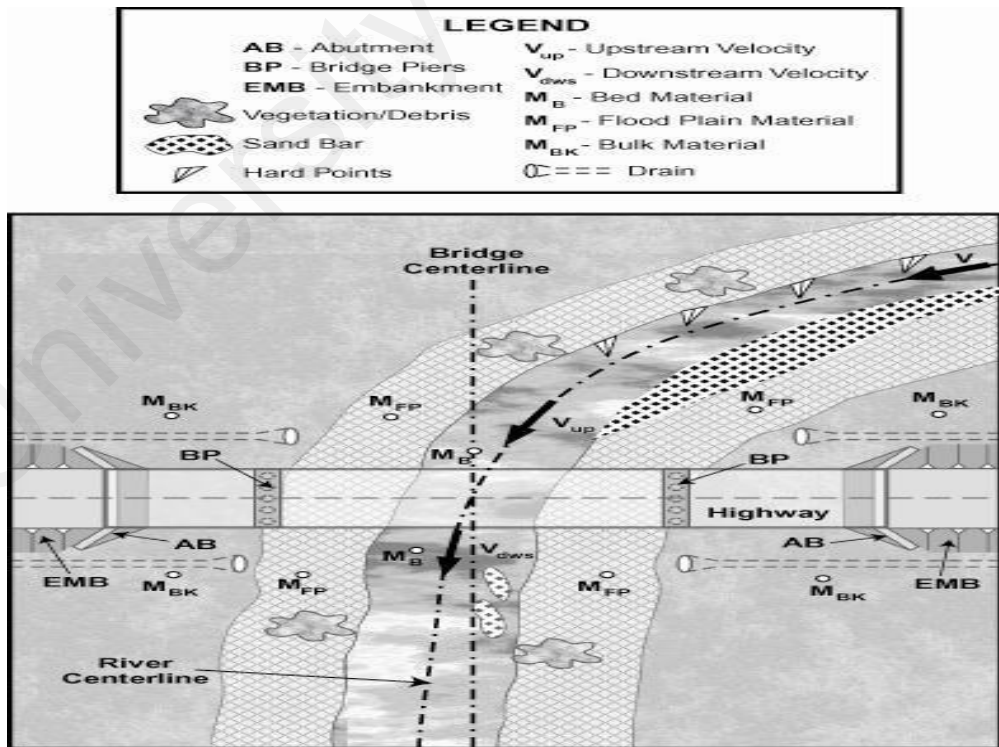


Figure 1.2: Sketch of bridge crossings during construction



Figure 1.3: A bridge failure in Wild River, Minnesota case caused by the interrelated action of scour and debris accumulation against the structure. (Ettema et al., 2006)

Inspection is used as a tool to detect any abnormalities to bridge including scouring. But it is impossible to conduct inspection to all bridges for scour. This conventional methods used to identify scour around bridge piers and abutments also cannot be used during high floods, when the maximum scour occurs. Thus, there is a need for an automated bridge scour monitoring system that can continuously monitor the scour depth around a bridge pier, especially under high flood conditions, and provide the bridge maintenance personnel an early warning system when scour reaches a critical depth. To address the critical need for a continuously monitoring bridge scour system, we intend to use spectral wavelength shift of Singlemode-Multimode-Singlemode (SMS) sensor to monitor local scour formation.

In this study, we will employ SMS interferometer to develop a robust system for continuous monitoring of the bridge scour. In order to achieve this goal, the sensitivity of the sensor package will be identified and subsequently analyzed to obtain a better understanding of this relatively new technology and then laboratory experiments will be

designed to test the performance and efficiency of this technology in continuous monitoring of the scour.

1.2. Singlemode-multimode-singlemode fiber (sms) structure

Lately, SMS structure has raised research interest due to having similar benefits to the fiber Bragg grating (FBG) on top of having its own advantages. The SMS structure has been exploited in many applications such as structural strain monitoring (Hatta, Semenova, Wu, & Farrell, 2010), displacement (Wu, Hatta, Wang, Semenova, & Farrell, 2010), pressure (Ruiz-Pérez, Basurto-Pensado, LiKamWa, Sánchez-Mondragón, & May-Arriola, 2011) and temperature sensors (Gao, Wang, Zhao, Meng, & Qu, 2010; Wu et al., 2010). It requires an easier and more economical device fabrication as compared to FBGs.

The structure can be easily built by fusion splicing a multimode fiber (MMF) between two single-mode fibers to form an interferometer structure. The transmission output produces a comb spectrum as a broadband light source is injected into the structure. Instead of having narrow spectral bandwidth as found in FBG, the output spectral is broader and exhibits an interference pattern at particular light wavelengths due to the interaction between multi-light propagation modes excited in the MMF section. Whenever strain or perturbation is applied at the MMF section, the spectral power and wavelength are changed accordingly which form the basis as a sensor device.

Up to date, there is no report on the application of SMS sensor in monitoring hydraulic systems such as local scour formation. Therefore, we demonstrate a local scour detection using an optical technique. For the SMS structure to be robustly responsive to water flow and able to withstand sediment movement, we propose a custom packaging method.

1.3. Problem Statement

Some problem such as scouring around bridge pier may lead to bridge collapsed and suspension of the piers. In some other causes, scouring at bridge piers may lead to bridge capacity and safety factors decrease. Piers scour led to decline in bridge capacity or safety factor. Much time, money and effort have been invested in the development of scour detection and instrumentation system to raise the safety concern. Hence, in this research which will be based on laboratory tests, cylindrical pier shape made of PVC pipe was used together with SMS sensor package to monitor the local scour phenomenon.

1.4. Research Aims and Objectives

The aim of this research is to develop a package sensor made from SMS structure to monitor the local scour at the bridge pier. The related objectives of the present research are as follows:

- a) To develop a SMS sensor package that has a water resist characteristic.
- b) To introduce the SMS as a scour sensor device.
- c) To measure the process of scouring/deposition using SMS fiber sensor by analyzing between three phases of scouring with wavelength shift.

1.5. Research Significance

If the findings of this research prove that SMS fiber sensor can be used as a scour sensor device, it will lead to imperative need as an automated bridge scour monitoring system that can continuously monitor the scour depth around a bridge pier, especially under high flood conditions. SMS fiber sensor requires an easier and more economical device fabrication as compared to FBGs. The structure also can be easily built. In

addition, it will be helpful for the bridge maintenance personnel to provide an early warning system when scour reaches a critical depth.

1.6. Organization of the Thesis

The first chapter is the introduction of the research. This chapter includes general of the research, bridge scouring, SMS sensor, problem statement, research aims and objectives, research significance, and organization of the thesis are briefly presented.

The second chapter covers the literature review that starts with introduction bridge problem in Malaysia, scour, factor influencing scour, specific parameters on local scour, predicting equilibrium scour depth, scour detection device consist of single mode fiber, multi-mode fiber and SMS sensor.

The third chapter presents the methodology and procedure for producing the SMS structure and sensor itself. This chapter also will present the procedure to conduct the scouring experimental complete with the materials used during experiment.

The fourth chapter presents the result and discussion of experimental investigation of the research.

The fifth chapter concludes the research findings. This chapter also gives recommendations for future studies.

CHAPTER 2: LITERATURE REVIEW

2.1. Bridge Problem in Malaysia

Problems in existing bridges in Malaysia are often variously identified by terms such as distress, defects, damage, deterioration and even bridge failure. When any of the bridge components fails to function as designed or intended, problems arise. Bridge normally fails due to problems in concrete members, problems in steel members, bearing problems, joint problems, hydraulic problems, excessive vibrations, impact of vehicles and vegetation growth (King & Mahamud, 2009). Scouring effect is one of the hydraulic problems that causes bridge failure in Malaysia. King & Mahamud (2009) had investigated several bridges that might have scouring of riverbed, either local scour around the piers or general scour that cause instability of bridge. The bridges include Sg. Jeniang, Kedah, Sg. Pukin, Pahang, Sg. Tempias, Sabah, Sg. Golok, Kelantan, Sg. Trolak, Perak, Sg. Keratong, Pahang, Sg. Gombak, Selangor, Sg. Plentong, Pahang, Sg. Kerayong, Kuala Lumpur and Sg. Salor, Kelantan. Fig. 2.1 shows the image of general scour of riverbed that occurring at Sg. Jeniang Kedah.



Figure 2.1: General scouring of riverbed at Sg.Jeniang

2.2. Scour

Scour is a natural phenomenon that occurs at the bridge pile when water flow with higher velocity attacks the pier bridge. Besides that, at the pile bridge, scour also can take place at the abutments, around spurs, jetties, and breakwater. The occurrence of local scour brings hazard to civil structures like bridges in many countries as it weakens the pier bridge causing it to collapse without warning (Bin Lin, Chang, Lai, & Wu, 2004; Bin Lin, Lai, Chang, & Li, 2006). Often, the scour is formed due to the river down-flow at the up-stream face of a pier and the formation of the horse-shoe vortex at the base of the pier (Akib, Mashodi, Jahangirzadeh, & Shirazi, 2013). Scouring happens due to the erosive behavior of flowing water on the bed and banks of alluvial channels. Flow near a bridge pier or abutment is attended by an enhanced sediment-carrying capacity. This may occur even when there is no transport of sediment away from the structure.

Scouring can cause catastrophic hazard by reducing support (Akib, Fayyadh, & Othman, 2011; Akib, Jahangirzadeh, & Basser, 2014; Akib, Liana Mamat, Basser, & Jahangirzadeh, 2014; Akib, Mohammadhassani, & Jahangirzadeh, 2014). This

phenomenon will bring to bridge failure. Bridge failure due to scour effect to the bridge pier is a significant cause and problem. This is a never ending problem. Much time, money and effort have been invested in the development of scour detection and instrumentation system to raise the safety concern.

There are three categories of scour which are general scour, contraction scour and local scour that may occur which will accelerate to bridge failure (Melville & Coleman, 2000). General scour happened when the sediment from the riverbed was removed from the flowing water. Contraction scour happen because of the increasing of the water velocity when the water flow through the bridge opening that is narrower than normal river channel. The sediment at the riverbed and sides will evacuate, this case we call it as contraction scour. Local scour occur due to hydraulic structure and develop by interactions between the flow and the obstacle for example bridge piers and abutments or spur dikes.

In this research, local scour is considered for experimental work. Local scour has two types which are, clear water scour, and live bed scour. Bridge scour is the one of the major factor that will cause the bridge to collapse. The estimation has been done where 60% of the scour will affect the bridge failure compare to the other related hydraulic causes. Figure 2.2 shows that the failure of the bridge due to scouring affects.

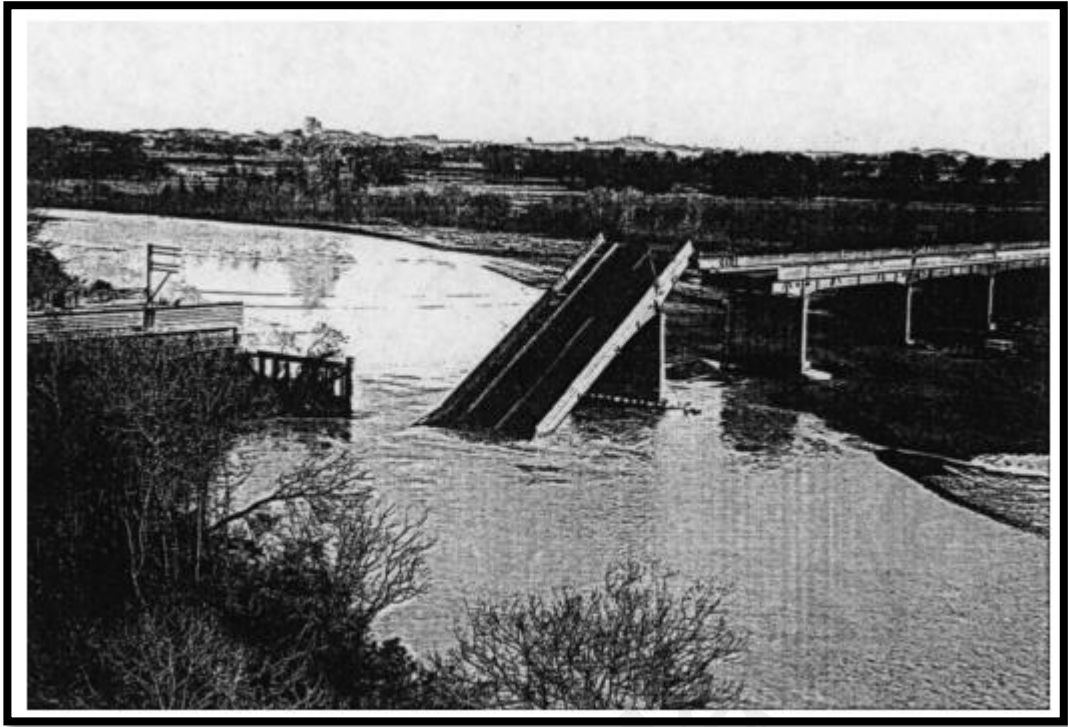


**Figure 2.2: Failure of Bulls Road Bridge, Rangitikei River, NZ, June 1973
(Melville & Coleman, 2000)**

Local scour will develop scour holes, which occur due to evacuation of the sediment around piers or abutments which follow the flowing stream. This evacuation happens due to a mix of the horseshoe vortex and down flow in front of the pier, whereas vortex shedding occurs at the back of the pier and the flow contraction (Moncada-M, Aguirre-Pe, Bolivar, & Flores, 2009). The mechanism of scour at a cylindrical pier is illustrated at Figure 2.3.

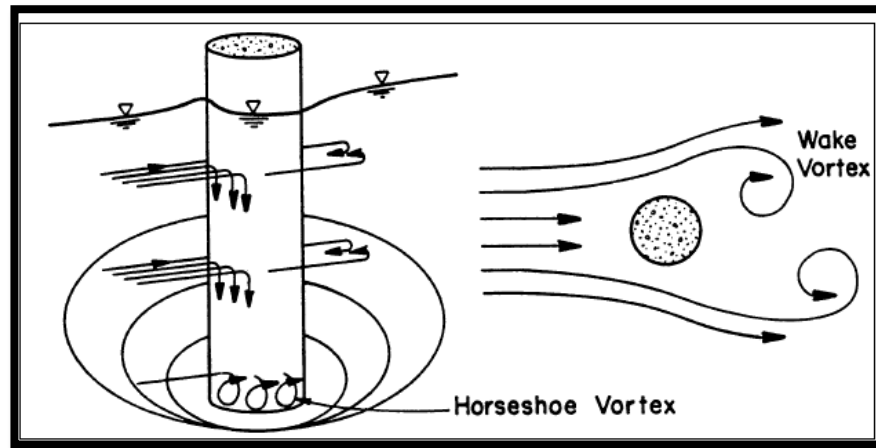


Figure 2.3: Scour at a cylindrical pier (Lagasse & Richardson, 2001)

2.2.1. Factors that influencing scour

As reported in the reference (Melville & Coleman, 2000), there are 5 factors that influence the bridge scour; geomorphic, flood flow transport, bed sediment, bridge geometric and scour protection measure.

Geomorphic factors influence both catchment and river characteristics. These factors are so crucial for a localized scour as compared to the general scour. The catchment characteristic is referred to the topographic, vegetative and soil characteristics, which is strongly influenced by the climatic change. River characteristics are related to valley setting, the channel cross-sectional shape, channel boundary properties and its platform shape. For valley setting can be refer to whether the river or let say the bridge is situated whether in flat, hilly or mountainous terrain. Deep-water channels can move significantly and unpredictably during floods in wide braided rivers.

Flood flow transport factors are related to sediment, water and debris transports, which are essential for determining local scour and general scour. Condition of live-bed or clear-water scour can be determined from the amount of sediment transport. Water

flow characteristics such as the spatial and temporal distributions of flow velocity and flow depth are determined by a flood flow hydrograph.

Bed sediment factors include particle size distribution and the spatial distribution. It is extremely complex phenomenon for scour that founded on cohesive soils. Scour of fine-grained soils cannot be evaluated on the basis of grain-size characteristics. This is due to the complex physiochemical interactions between colloidal particles, the effects of preloading and the effects of pore water pressures. Probable limit for bridge foundation depth can be determined from bed rock level.

Bridge geometric factors could be used to examine the local scour. These factors include the degree of flow contraction caused by the bridge restricting the flow area, the foundation geometry, and the presence of scour protection works and the sitting of the bridge in relation to channels bends. This factor influencing bridges scour can be described by several characters, which are the type, shape, width, length and alignment with the flow of individual piers. The position of piers and abutment in the river channel also can be classified as an important factor. Piers that located near to an abutment must have attention because they can experience deeper scour, being subject to the flow near the abutment. Also, piers that placed at the edge of the main channel can experience significant lateral flow and causes to deeper scour because of the associated skewness of the flow.

Scour protection measures can be classified according to the type of scour that they wish to control. Revetment such as riprap, retards such as willow planting, spurs, dikes, spur dykes, hard points and jack or tetrahedron fields are the lateral bank control countermeasures (Melville & Coleman, 2000). Check dams and local protection at piers and abutments can control degradation. Whereas, for aggradations control measures,

include various river channel works and compensate for reduced flow area by widening of the bridge opening or rising of the bridge.

2.2.2. Specific parameters on local scour

Several parameters have been identified to determine the maximum scour depth at bridge piers in the laboratory experiment. These parameters affect the data collected in laboratory work and they are briefly described in this subsection.

The process of scouring under clear-water condition establishes asymptotical effect towards the equilibrium depth of scour. For instance, under live-bed conditions, the equilibrium depth is reached at a faster time and the scour depth oscillates due to the passage of bed features past the piers or abutment. Melville (2008) reported that the equilibrium conditions was achieved in lesser time and the duration of the scour activity does influence the scour depths. The scour depths was obtained at less than 50% of the equilibrium depth in a short period of the experiment (10 to 12 hours) (Melville, Parola, & Coleman, 2008).

Flow shallowness, y/B shows effects of the depth of flow. Thus flow is in relation to the pier width, B or projected length of abutment (including the approach embankment) (Melville & Coleman, 2000). Useful classification of scour process at the bridge foundation can be obtained from the ratio of B/y where B is pier width and y is flow depth. Table 2.1 shows the classification of local scour processes at bridge foundations gained from the derivation of the laboratory data plotted. The data also determine the functional relations, $d_s = f(B, y)$ and d_s is scour depth, described the influenced of flow shallowness on local scour depth.

Table 2.1: Classification of local scour process at bridge foundations

| Class | B/y | Local Scour Dependence |
|--------------------|-----------------|--------------------------|
| Narrow | $B/y < 0.7$ | $d_s \propto B$ |
| Intermediate width | $0.7 < B/y < 5$ | $d_s \propto (By)^{0.5}$ |
| Wide | $B/y > 5$ | $d_s \propto y$ |

Depths of local scour are not affected by the sediment coarseness, B/d_{50} for the uniform sediments, unless the sediment is relatively large. Local scour depth is influenced by sediment size proved by the laboratory data which is when $B/d_{50} < 50$ as shown in Figure 2.4.

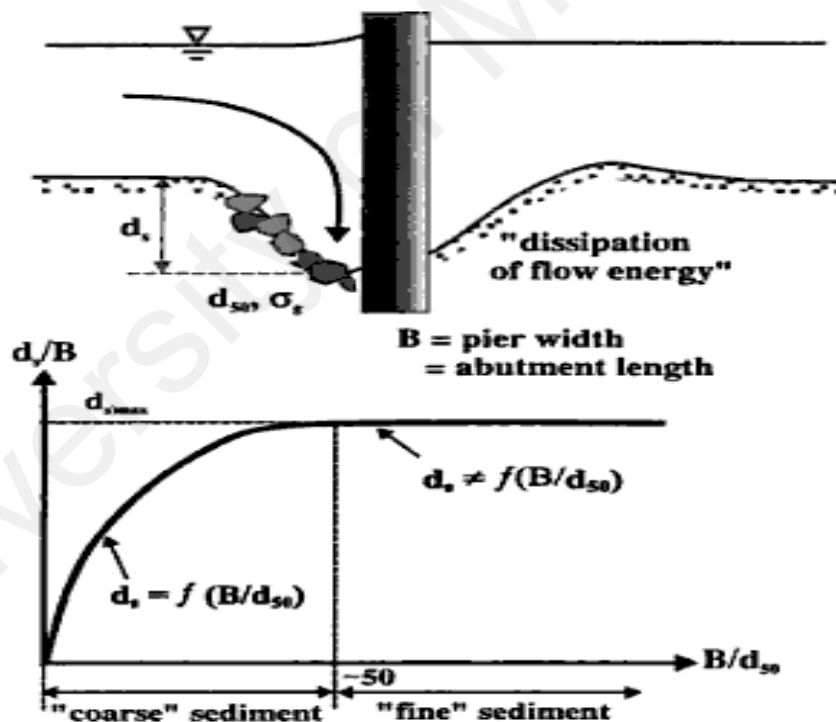


Figure 2.4: Local scour depth variation with sediment coarseness (Melville & Coleman, 2000)

Around the threshold condition, $V/V_c = 1$, on the approach flow bed and at the base of the scour depth armoring will occur. Figure 2.5 shows the pattern evident from these studies.

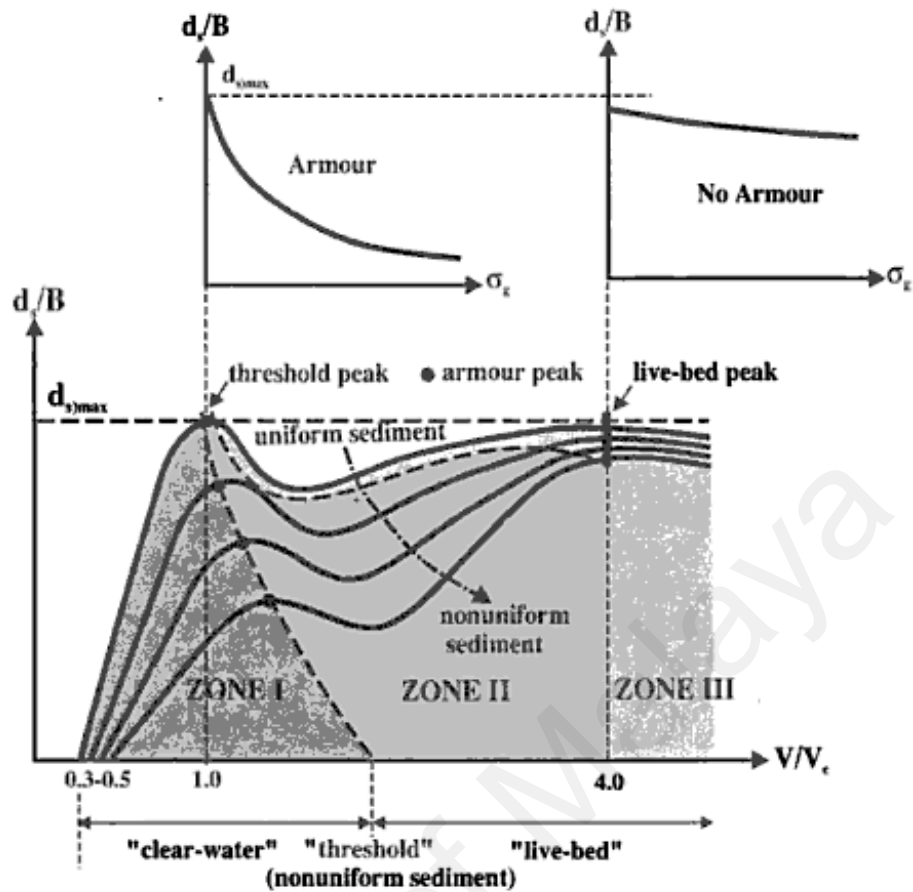


Figure 2.5: Local scour depth variation with sediment non-uniformity (Melville & Coleman, 2000)

2.2.3. Effect of flow intensity, V/V_c

Scour can be classified into two types; live-bed and clear-water scours. Live-bed scour involves the mobilization of bed material. Clear-water scour occurs when there is no accumulation of the bed material. It occurs when the shear stress induced by the water flow exceeds the critical shear stress of the bed material. During a high density, river volume such as flood, bridges with streams that contain over coarse-bed material are often subjected to clear-water scour at low discharges, live-bed scour at the higher discharges and then clear-water scour at the lower discharges on the falling stages. Figure 2.6 shows pier scour depth against time in a sand-bed for both types of scours. As shown in the figure, clear-water scour reaches its peak over a longer period of time than live-bed scour.

This is due to clear-water scour that occurs mainly in coarse-bed material streams. In practical, after several floods, the local clear-water scour may not reach the maximum depth. It is shown that the maximum local clear-water pier scour is about 10 percent greater than the equilibrium local live-bed pier scour.

Clear water scour happens for uniform and non-uniform sediments when flow intensity, $V/V_c < 1$ and $[V - (V_a - V_c)] / V_c < 1$ respectively (Melville & Coleman, 2000). This condition present, where V_a is the mean approach velocity at the armor peak. In the case of live bed scour for uniform sediments, critical velocity, V_c is lower than the mean approach velocity ($V/V_c > 1$) This is shown that live bed scours recovers only for uniform sediment when geometric standard deviation of particle size distribution less than 1.

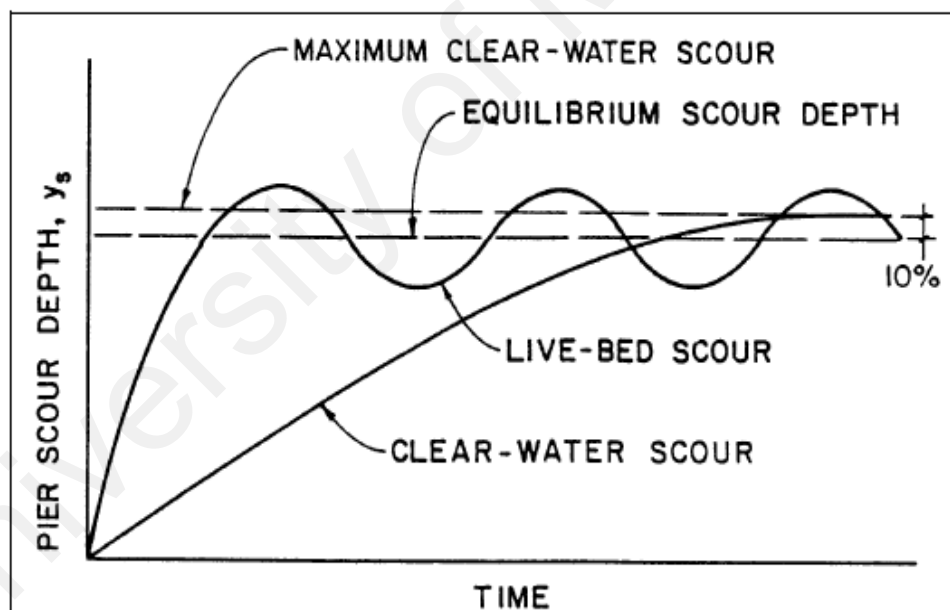


Figure 2.6: Pier scour depth in a sand-bed (Lagasse & Richardson, 2001)

Water depth, flow angle and strength, materials properties of the sediment, pier and abutment shape and width, and so on are the highlighted factors that can cause this dynamic phenomenon (Deng & Cai, 2009) .

2.2.4. Predicting Equilibrium Scour depth

The information gathered from the factors influencing scour depth could be used to predict the scour bridge. Scour prediction can be obtained generally by two approaches: empirical equations and neural networks (Deng & Cai, 2009). However, it was reported that the equilibrium scour depth cannot be specified for experiments shorter than one to two weeks (Simarro, Fael, & Cardoso, 2011). Other reports also mentioned that prediction of local scour depth is difficult since the mechanism of scouring at a pile group is quite complex due to the high 3-dimensionality of the flow (Lança, Fael, & Cardoso, 2010), (Amini, Melville, Ali, & Ghazali, 2011). The equilibrium scour depth is also very slow to be obtained in clear-water scour condition. This is due to during equilibrium time, rate of sediment transported out and in from hole is same and under clear-water condition, pier foundation is eroded rapidly at the early stage but, subsequently scour hole development reached equilibrium as the magnitude of the stresses is reduced due to the flow alteration caused by the generation of scour hole.

2.3. Scour Detection Device

Recently, many method such as sonar (De Falco & Mele, 2002; Hunt, 2005), radar (Anderson, Ismael, & Thitimakorn, 2007; Forde et al., 1999), time-domain reflectometry (TDR) (Yankielun & Zabilansky, 1999; Yu & Zabilansky, 2006) and fiber-Bragg grating (FBG) (Lin, Chen, Chang, Chern, & Lai, 2005; Xiong, Cai, & Kong, 2012; Z. Zhou, Huang, Huang, Ou, & Chen, 2011) have been developed to monitor local scour. Apparently, the main drawback of sonar and radar methods is due to the difficulty in interpreting results corrupted by noises coming from mud, rocks, and debris flowing in the river water when flooding occurs. On the other hand, the TDR technique suffers from the electromagnetic field interference (EMI), signal attenuation and pulse dispersion due to having long distance cable. Therefore, the FBG technique has been proposed and

demonstrated to resolve the issues associated with the methods above. It offers immunity to electrical noise and EMI, provides high sensitivity resolution, compactness and structural compatibility.

Lately, singlemode-multimode-singlemode fiber (SMS) structure has raised research interest due to having similar benefits to the FBG on top of having its own advantages. The SMS structure has been exploited in many applications such as structural strain monitoring (Hatta, Semenova, Wu, & Farrell, 2010), displacement (Wu, Hatta, Wang, Semenova, & Farrell, 2010), pressure (Ruiz-Pérez, Basurto-Pensado, LiKamWa, Sánchez-Mondragón, & May-Arrijoja, 2011) and temperature sensors (Gao, Wang, Zhao, Meng, & Qu, 2010) (Wu et al., 2010). It requires an easier and more economical device fabrication as compared to FBGs. The structure can be easily built by fusion splicing a multimode fiber (MMF) between two single-mode fibers (SMF) to form an interferometer structure. In this work, a SMS structure is proposed to detect and measure the scour.

2.4. Singlemode-Multimode-Singlemode (SMS) Structure

SMF normally has a core diameter of within 8.3 to 10 microns and thus allows only one mode of transmission. It is made of a single strand of glass fiber. In communication, the SMF has a cutoff wavelength of around 1200 nm and thus it could operate in single mode regime with 1310 and 1550 nm light source. SMF is used to avoid modal dispersion and thus it carries higher bandwidth than MMF, but needs a light source with a narrow spectral width. The small core and single light-wave virtually eliminate any distortion that could result from overlapping light pulses, providing the least signal attenuation and the highest transmission speeds of any fiber cable type.

Same as the SMF, MMF is also made of glass fibers. It has core diameter in a range from 50 to 100 micron. Typical multimode fiber core diameters are 50, 62.5, and

100 micrometers. Light waves operating at 850 or 1300nm are dispersed into numerous modes, or paths, as they travel through the MMF's core. However, in long distance transmission, multiple paths of light can cause signal distortion at the receiving end, resulting in an unclear and incomplete data transmission.

A single mode–multimode–single mode (SMS) fiber structure has been proposed as a strain sensor as it generates a sufficient bandpass spectral response for a given wavelength range (Wu et al., 2010; D.-P. Zhou, Wei, Liu, & Lit, 2009). It can be used as either a stand-alone sensor or an edge filter that interrogates an optical sensor such as an FBG. Since an SMS fiber structure is much easier to fabricate than an FBG, a sensor based on an SMS fiber structure will be more economical than the one based on an FBG. A straight SMS fiber structure can be used as a load sensor, but just like an FBG sensor, a straight SMS structure suffers from a narrow measurement range, due to the limited strain that can be applied to avoid breaking it.

The transmission output produces a comb spectrum as a broadband light source is injected into the structure. Instead of having narrow spectral bandwidth as found in FBG, the output spectral is broader and exhibits an interference pattern at particular light wavelengths due to the interaction between multi-light propagation modes excited in the MMF section. Whenever strain or perturbation is applied at the MMF section, the spectral power and wavelength are changed accordingly which form the basis as a sensor device.

Up to date, there is no report on the application of SMS sensor in monitoring hydraulic systems such as local scour formation. Therefore, we demonstrate a local scour detection using an optical technique. To the best of our knowledge this might well be the first attempt on the use of SMS interferometer to monitor local scour formation on a PVC pipe. This preliminary study is useful to investigate possible effects of scour formation on real bridge piers.

2.5. Summary

From this review can concluded that this attractiveness of the SMS device is not only in its sensitivity but also as it provides simpler and cheaper fabrication method as compared to FBGs. The structure can be easily built to produce a bandpass interferometer spectral output when broadband light source is injected into the structure. Whenever strain or enough heat is applied at the MMF section, the spectral power and wavelength are changed which form the basis as a sensor device. The importance of developing SMS sensor to detect local scour is beneficial in civil applications. As scour often bring many important structures such as bridges to collapse during flooding. Thus, there is a need to develop a sensor system to raise safety concern.

CHAPTER 3: MATERIALS AND METHODS

3.1. Introduction

This chapter briefly describes on both material and equipment used in this work as well as the research methodology. The condition of the materials and the procedure followed in conducting the laboratory experiments are also explained in this chapter. All experiments were conducted at the Photonics Research Centre and Hydraulics Laboratory at Faculty of Engineering, University of Malaya. Scour experiments in this research work were conducted based on Melville and Coleman's methods.

3.2. Materials And Equipment

3.2.1. Optical Fiber

Fiber-optic plays an important role in the world scientific advancements especially in telecommunication industry. Many works have been reported, and many products have be manufactured based on fiber-optic technology, offering diverse benefits to our modern society. Besides telecommunications, optical fibers are also used in sensors; research in fiber-optics sensors have produced new sensor applications as well as brought better solutions to existing sensing problems. Optical fibers are a kind of waveguides, which are usually made of some kind of glass, can potentially be very long (hundreds of kilometers), and are in contrast to other waveguides fairly flexible. Silica glass is widely used for fabrication optical fibers because of its outstanding properties such as extremely low propagation losses and high mechanical strength against pulling and even bending.

Fig. 3.1 shows a typical optical fiber structure, which consists of a glass core surrounded by a transparent cladding material with a lower index of refraction. A polymer jacket is used to protect the glass core and cladding sections. The light propagates along

the core based on total internal reflection principle. The index contrast between core and cladding is typically very small and it determines the numerical aperture and single mode operation of the fiber. Light launched into the fiber propagates mainly in the core region, although the intensity distribution may extend somewhat beyond the core. Due to the guidance and the low propagation losses, the optical intensity can be maintained over long lengths of fiber. The light can also be guided inside the fiber using a principle of photonic bandgap, which can be realized using a modern optical fibers such as Bragg fiber and photonic crystal fibers.

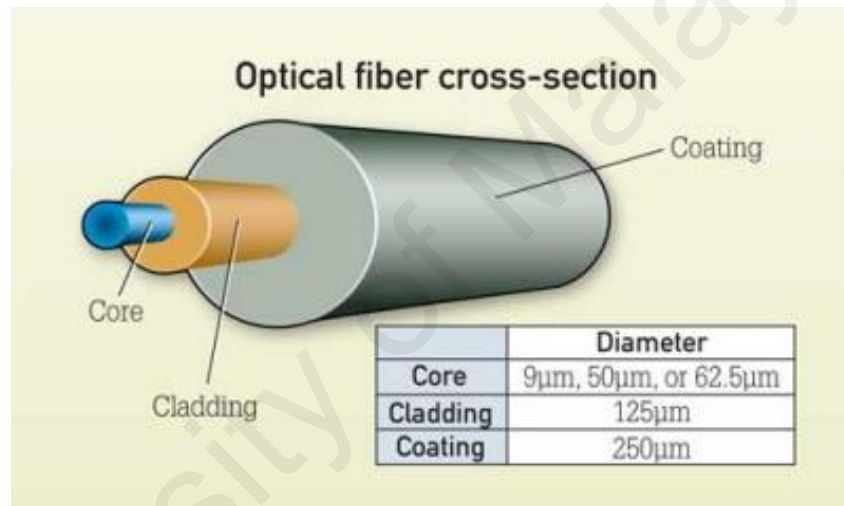
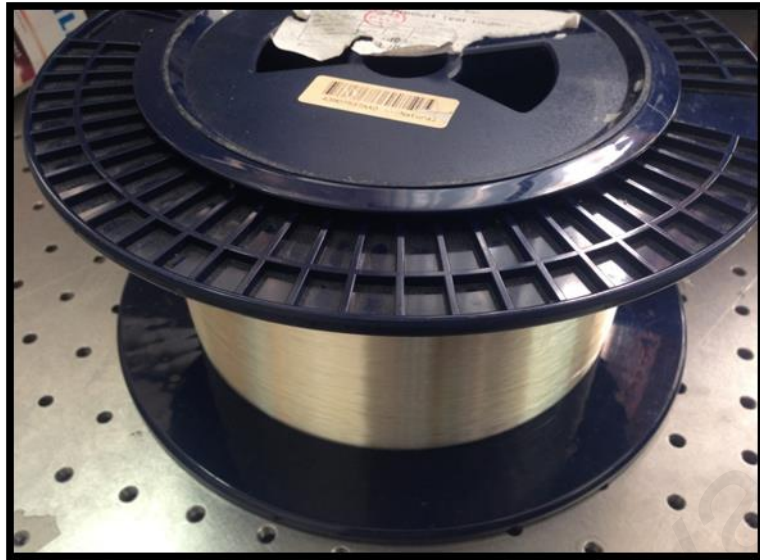


Figure 3.1: Optical fiber structure

The simplest fiber is a step-index fiber, where the refractive index is constant within the core and within the cladding. In this work, a standard single-mode fiber (SMF) and multi-mode fiber (MMF) are used in the fabrication of the sensor probe. Both SMF and MMF have a step-index profile with a core diameter of 9 μm and 50 μm , respectively. Figs. 3.2 (a) and (b) shows the image of the SMF and MMF spool used in this work, respectively.



(a) SMF spool



(b) MMF spool

Figure 3.2: Images of the commercial fibers used in the experiment (a) SMF (b) MMF.

3.2.2. Fusion Splicer

In this dissertation, Fujikura Arc Fusion Splice FSM-50S was used to fabricate the proposed SMF-MMF-SMF structure, which functions as a sensor probe. This kind of fusion splicer has been designed for splicing many types of optical fibers such as SMF, MMF, Erbium-doped fiber, dispersion shifted fiber etc. The splicer device is small in size and light in weight, making it suitable for any operating environment. It is easy to operate

and it splices fast while maintaining low splicing loss. The splicing loss for splicing SMF and MMF is maintained less than 0.1 dB throughout our experiment. The image of the splicer is shown in Fig. 3.3.



Figure 3.3: Fujikura Arc Fusion Splicer (a) outside view (b) screen view

3.2.3. Optical Spectrum Analyzer

An Optical Spectrum Analyzer (OSA) is a precision instrument to displays and measures the distribution of power of an optical source over a specified wavelength span. An OSA traces displays power in the vertical scale and the wavelength in the horizontal scale. In this experiment, an Optical Spectrum Analyzer from Anritsu model MS9710C (Fig. 3.4) was used to analyze the output spectrum from the sensor probe. This MS9710C OSA is a diffraction-grating based spectrum analyser, which is capable to analyse optical spectrum in the wavelength range from 600 to 1750 nm.



Figure 3.4: Anritsu Optical Spectrum Analyzer used in this work

3.2.4. Amplified Spontaneous Emission (ASE) Light Source

The Amplified Spontaneous Emission (ASE) Light Sources is a stable and high power broadband sources designed for optical measuring and testing applications. The ASE is obtained by pumping a piece of Erbium-doped fiber (EDF) with a 980 nm laser diode. The pumping excites Erbium ions to move an excited state and create a population inversion. The spontaneous emission from the Erbium ions is amplified along the fiber to produce ASE light operating in C-band region. The broad spectrum width for the ASE light source is ideal for applications in Dense Wavelength Division Multiplexing (DWDM) systems, sensor systems and components characterization.

3.2.5. Pier Model

Figure 3.5 shows the PVC pipe which is attached to a wooden support structure via screw and metal plating. The PVC pipe has a diameter of 20 mm and length of 500 mm. The vertical scale was fixed at the pipe to ease reading of scour depth measurements.



Figure 3.5: Pier model made of PVC pipe

3.2.6. Coarse Sand

Coarse sand was selected to imitate the granular backfill that surrounded the bridge piers on control block in real conditions. Figure 3.6 shows the image of coarse sand used in the experiments. The type of sand used was based on a suitable scale of the pier model. The coarse sand filled to a flat full level in the control block inside the test flume. The sand in the control block was compacted to ensure the adequate uniformity. From the removal of coarse sand surround the bridge piles, the scour depths caused by the different velocities of water flow were measured. Characteristic of bed sediment is uniform. The specific gravity of the sediment is 2.65 for particle size of 0.8 mm and geometric standard is 1.29 (Akib, Othman, Othman, Amini, & Marzuki, 2009). This value was used to tabulate the spring stiffness value of structural support on the piles.



Figure 3.6: Coarse sand used in the experiments

3.2.7. Control Block

Figure 3.7 shows a control block used during the hydraulic experiment. It has a height of 200 mm and was placed inside the test flume. The pier model was put in between the control block. The control block was then filled flat full level with the bed sediment. There is only 50 mm height of bed sediment filled outside of the control block. This control block is used to reduce the usage of bed sediment and to avoid filling of the whole flume with sand along the 16 m of the flume channel with 200 mm height of bed sediment. The control block used in this experiment has a thickness of 20 mm.



Figure 3.7: Control block used during the hydraulic experiment

3.2.8. Hydraulic Flume

Hydraulic flume (Figure 3.8) is a river laboratory model to control the parameters of the flow for the research purpose. The parameters are flow and water level to measure scouring. Hydraulic flume is located in the hydraulic laboratory of University of Malaya. It has a length of 16 m, 1 m width and 1 m depth having a constant longitudinal slope of 0.001. The water level of flume is set in the range of 350 mm – 355 mm to represent the flooding conditions. The opening gauge (Figure: 3.9) was set at a certain height to get the required water flow levels and to control the water level and velocity. After the water flow stabilized in allowable range of water level fluctuation, the water pump was turned on to get the desired area flow velocity. Water pump was controlled by a system based on InduSoft (Figure 3.10).



Figure 3.8: Hydraulic Flume



Figure 3.9: Opening Gauge of the flume

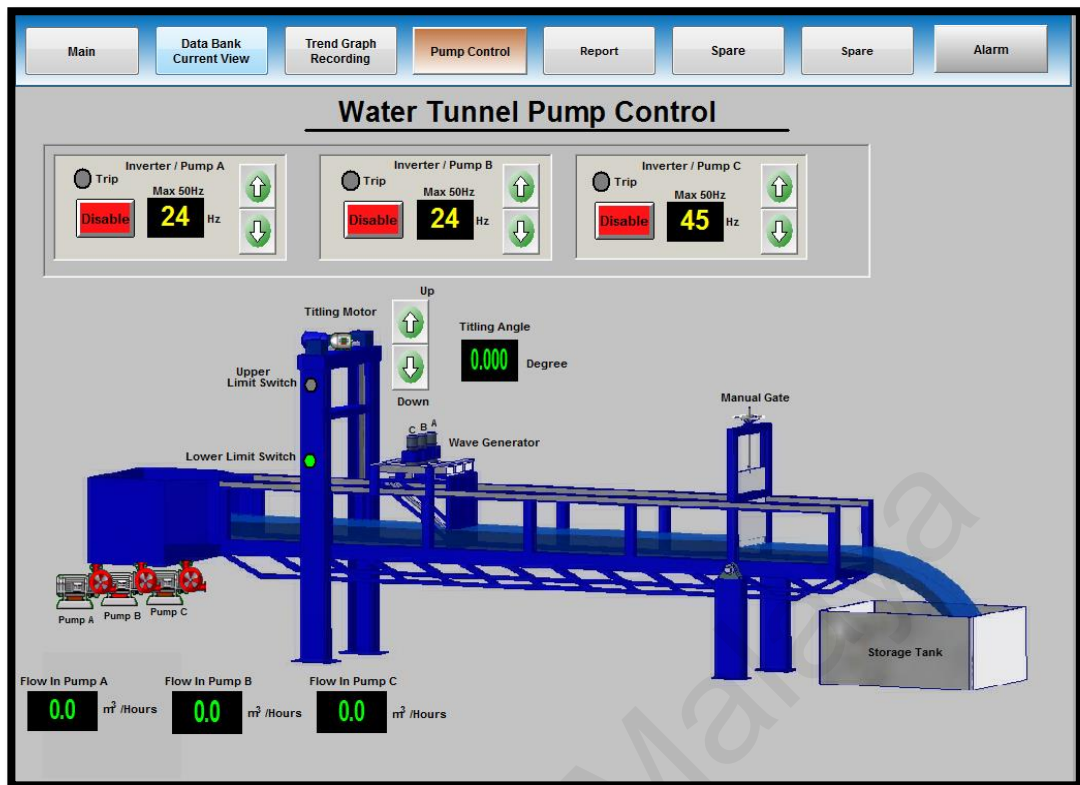


Figure 3.10: Graphic user interface of the InduSoft Software, which is used to control water flow into hydraulic flume

3.2.9. Water Condition

The water in the flume should be as clear as possible, so that scour depth reading could be taken easily. Furthermore, the water should not contain any significant solid material that will cause sediment on the flume and model. In the experiment, the water temperature should be kept at room temperature to imitate the site temperature in Malaysia.

3.3. Research Methodology

The experimental investigation started with preparation of the sensor where a fiber is spliced to develop the SMS structure. Next step is to put the structure into package. An experimental investigation was conducted in a flume of 16m in length, 1m width, and 1m depth flume with constant longitudinal slope of 0.001. The experimental work was then conducted to study and measure the scour depth using an optical probe at a bridge piers, which was simulated using a PVC pipe model. Scour depths were measured as a function of discharge and sediment size.

3.3.1. Splicing Fiber

Fusion splicing is actually a process of joining two optical fibers using heat induced by fusion action. The aim is to fuse end-to-end fibers together so that the light can pass through the joint with minimum scattering and back-reflection losses. Figure 3.11 shows the step in splicing two fibers. At first, a fiber was cut to a desired length. In this experiment, multi-mode fiber used is 4.9 cm. Then, the protective polymer coating around optical fiber was removed by using wire-stripper. This step is called a stripping step. Once the protective coating layer removed, the bare fiber needs to be cleaned using alcohol and wipes. The clean end fiber is then cleaved using the score-and-break method based on a commercial fiber cleaver. This is to ensure that its end-face is perfectly flat and perpendicular to the axis of the fiber. The cleaved fiber is then spliced with another fiber using the Fujikura Arc Fusion Splicer. The estimated splice loss is displayed upon completion of splicing. In this experiment, the splice loss was controlled to be less than 0.1 dB.

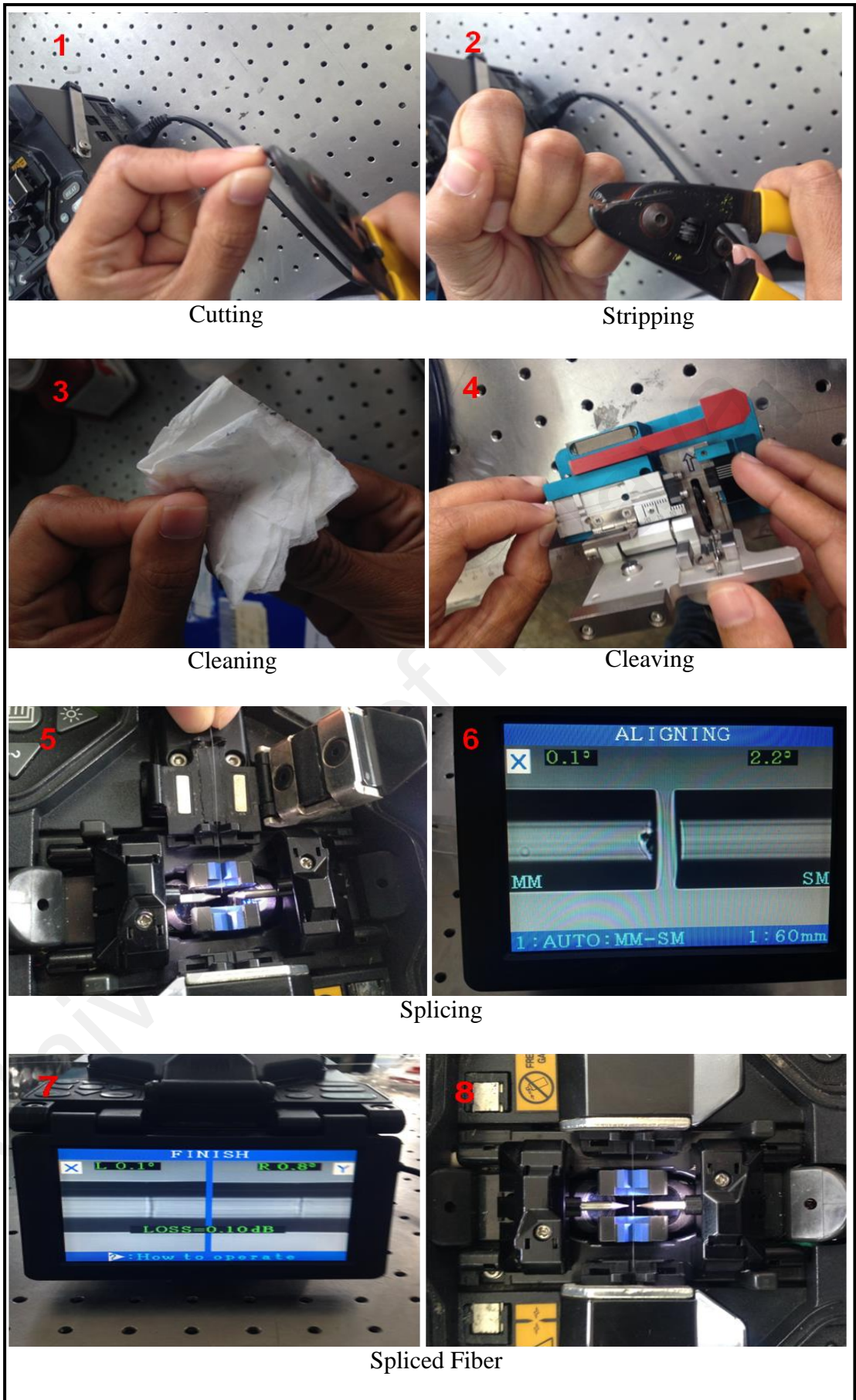


Figure 3.11: Steps of splicing fiber

3.3.2. Singlemode-Multimode-Singlemode (SMS) Sensor Package

The sensor probe in this dissertation is based on single-mode multimode single-mode (SMS) fiber structure. This structure should be designed, fabricated and packaged so that it can robustly responsive to water flow and able to withstand sediment movement. A custom packaging method was proposed as illustrated in Figs. 3.12 (a)-(d). At first a MMF with a step index profile, core size of 105 μm and a length of 4.9 cm is spliced between two SMF-28 fibers to construct the SMS structure. Then, the entire SMS structure is placed on the Cr-39 plastic monomer plate with the centre of the MMF coincides with that of the plate as shown in Fig. 3.12 (a). Tapes were used to attach and hold the SMS fiber to the plate. The elastic and flexible Cr-39 plate has length of 17.5 cm, width of 4 cm and thickness of 0.05 cm. The plate is securely placed on a flat and solid surface to avoid unnecessary displacement during the whole packaging process. To permanently attach the fiber to the plate, a small amount of water -proof epoxy was spread thinly and evenly over the fiber using a mini spatula as depicted in Fig 3.12(b). Afterwards, a blow dryer was used to dry and harden the epoxy for a duration of 5 minutes before it was left to dry for another 10 minutes. During the process, the SMS fiber was adjusted accordingly by pulling the fiber end to make sure the SMS fiber was straight and aligned properly. Then, another Cr-39 plate with the same dimension was used to cover the whole SMS structure on top of the other plate. The plates were pressed together and left to dry for 3 hours to ensure maximum adhesion for the SMS structure as shown in Fig. 3.12(d). Fig. 3.13 shows the image of the packaged SMS structure.

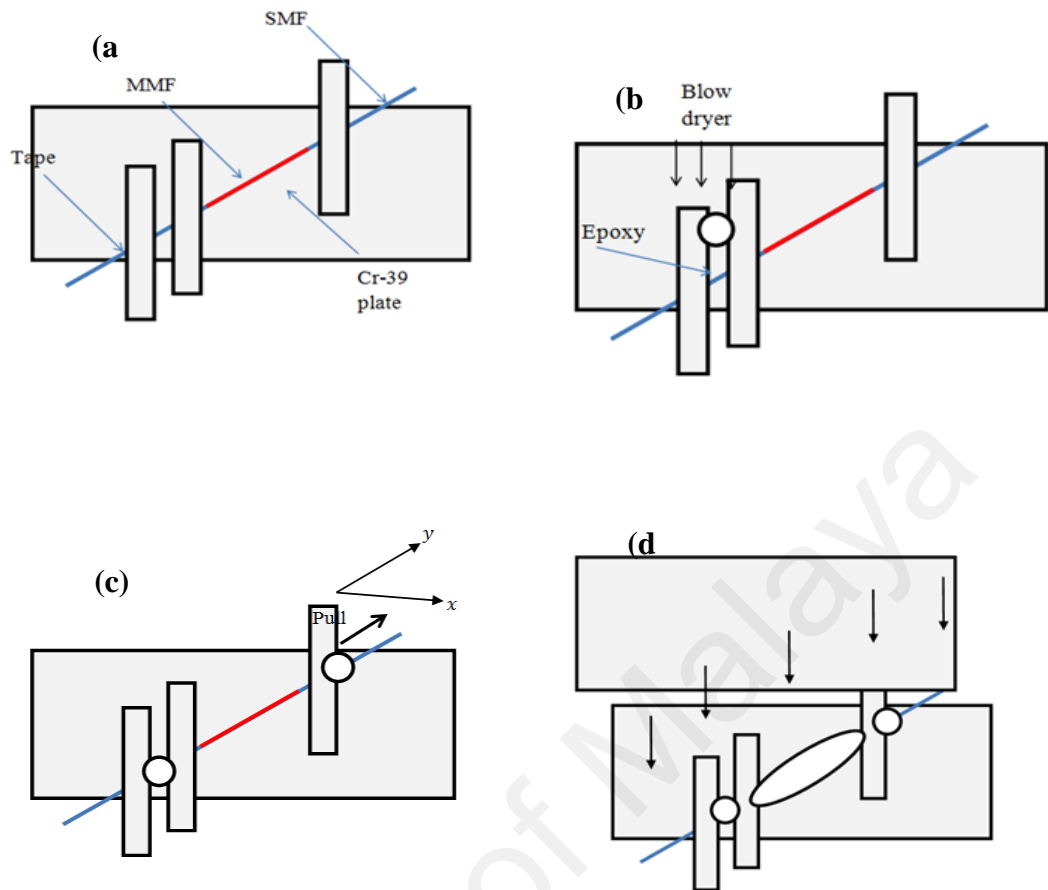


Figure 3.12: Stages to package the SMS Sensor

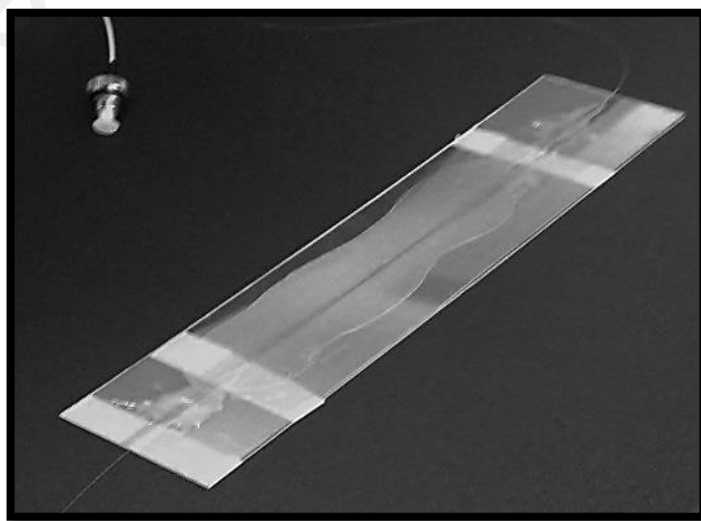


Figure 3.13: SMS sensor package

3.3.3. Sensor installation and experimental setup

Figure 3.14 shows the experimental setup of the local scour monitoring on a PVC pipe using the packaged SMS structure. The PVC pipe is attached to a wooden support structure via screw and metal plating. It has a diameter of 20 mm and length of 500 mm. A depth meter is attached to the pipe to measure the scour depth. The installation of the sensor is shown in Figure 3.15 as well. The sensor is attached to a concrete block of 50 mm x 50 mm x 50mm using water proof epoxy. A passage is built underneath the block for the fiber line from the bottom part of the sensor to pass through and enter the lower opening of the PVC pipe. It goes up to the top of the PVC pipe and is terminated at an FC/PC connector. The connector is linked to a 3 km long SMF 28 fiber before ending at an ASE source. The other fiber end of the sensor which acts as the output terminal is also connected to a FC/PC connector at the top of the PVC pipe. An optical spectrum analyzer (OSA) is connected to the output connector via a 3 km long SMF-28 fiber. Any excess fiber from the input or output side of the sensor is looped around and attached to the PVC pipe using tapes and cable ties.

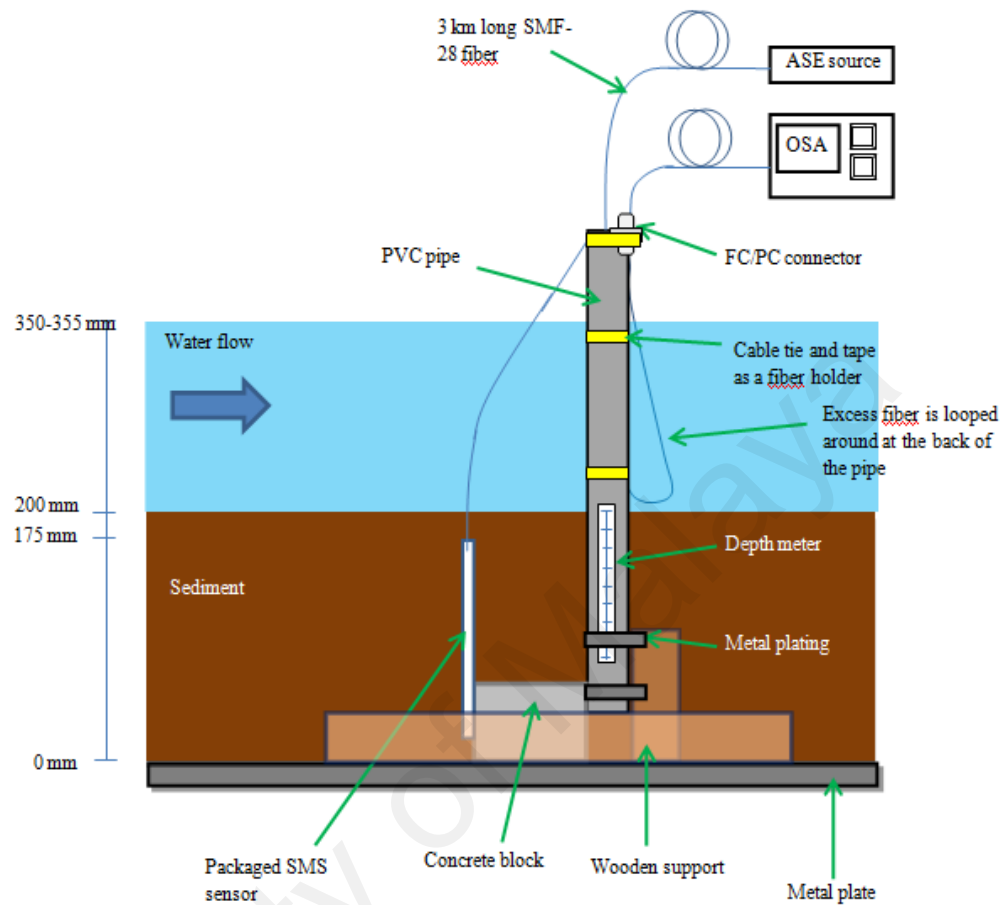


Figure 3.14: Installation of the package SMS structure for local scour monitoring on a PVC pipe.

The sensor and PVC pipe assembly is placed into the base of hydraulic flume (Fig. 3.15 (a)). It has a length, width and depth of 16 m, 1 m and 1 m, respectively with a constant longitudinal slope of 0.001. The assembly is placed evenly flat on the surface of the metal platform or the base of the flume prior to sediment piling. Non-cohesive, uniform sediment with median particle size of 0.8 mm, geometric standard of 1.29 and specific gravity of 2.65 is piled in the flume at a depth of 200 mm that spans across the center location of the flume at 4 meter long. Control blocks are placed at the front and the back of the bed material to avoid filling the whole flume with sediment. Additional sediment is also piled at a 50 mm depth and 0.2 m length just outside the blocks. Figure

3.15 (b) shows the photo image of the sediment piling around the PVC assembly with the sensor head located below the sand level. On the other hand, Figure 3.15 (c) shows the sediment leveling and distribution to achieve a depth of 200 mm inside the control block and 50 mm outside the control block. Figure 3.15 (d) shows the model in flume before experiment start.

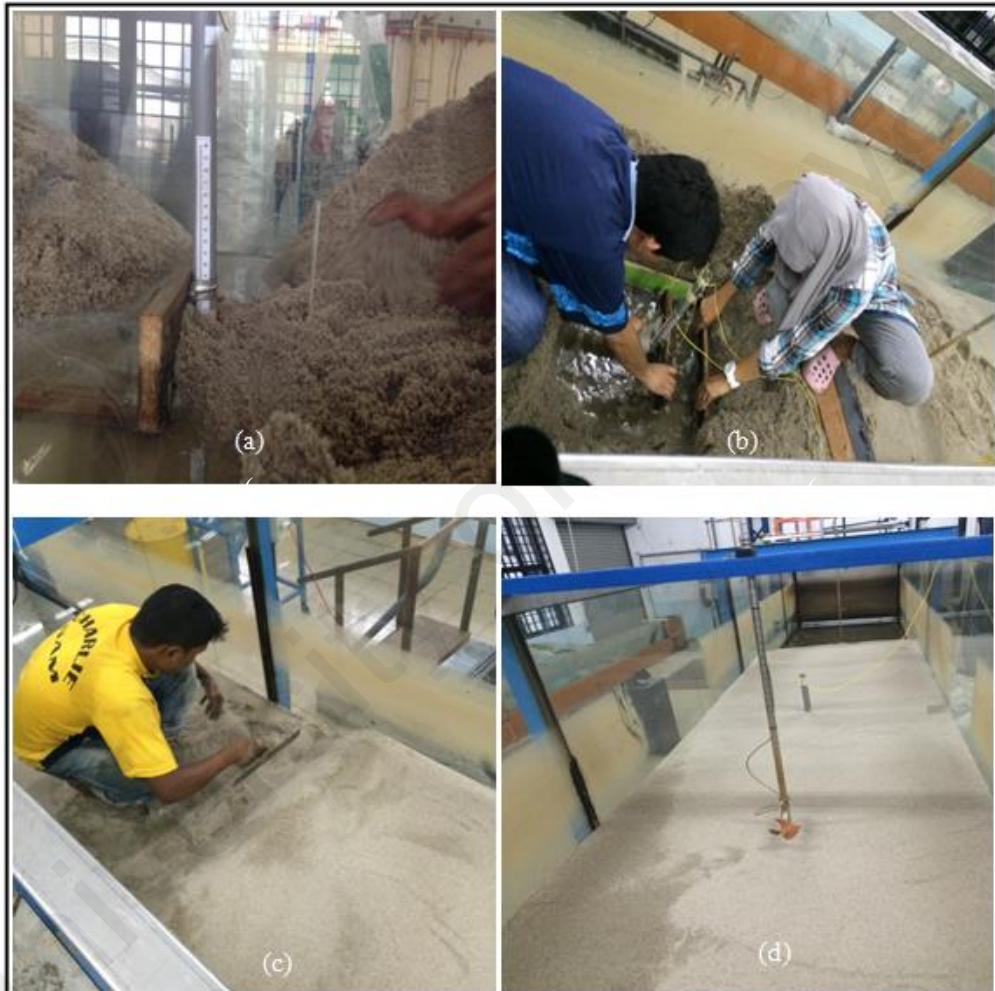


Figure 3.15: Photo images of (a) – (b) Sediment piling at the sensor and PVC assembly. (c) Process of leveling and distribution of sediment and (d) model in flume before experiment start

After the sediment piling process is complete, water flow is discharged at a direction shown in Figure 3.16 with an upstream velocity of 0.34m/s, and at flow depth of 350–355 mm to represent flooding conditions. The scour depth and spectral

measurements are recorded at different time interval with a sediment depth of 150 mm as an initial value. The scour depth and dimensionless scour depth are calculated from the following equations for the analysis,

$$\text{scour depth, } ds = \text{Initial Depth} - \text{Depth observed} \quad (1) \quad 3.1$$

$$\text{Dimensionless scour depth} = \frac{\text{scour depth, } ds}{\text{pier width, } B} \quad (2) \quad 3.2$$

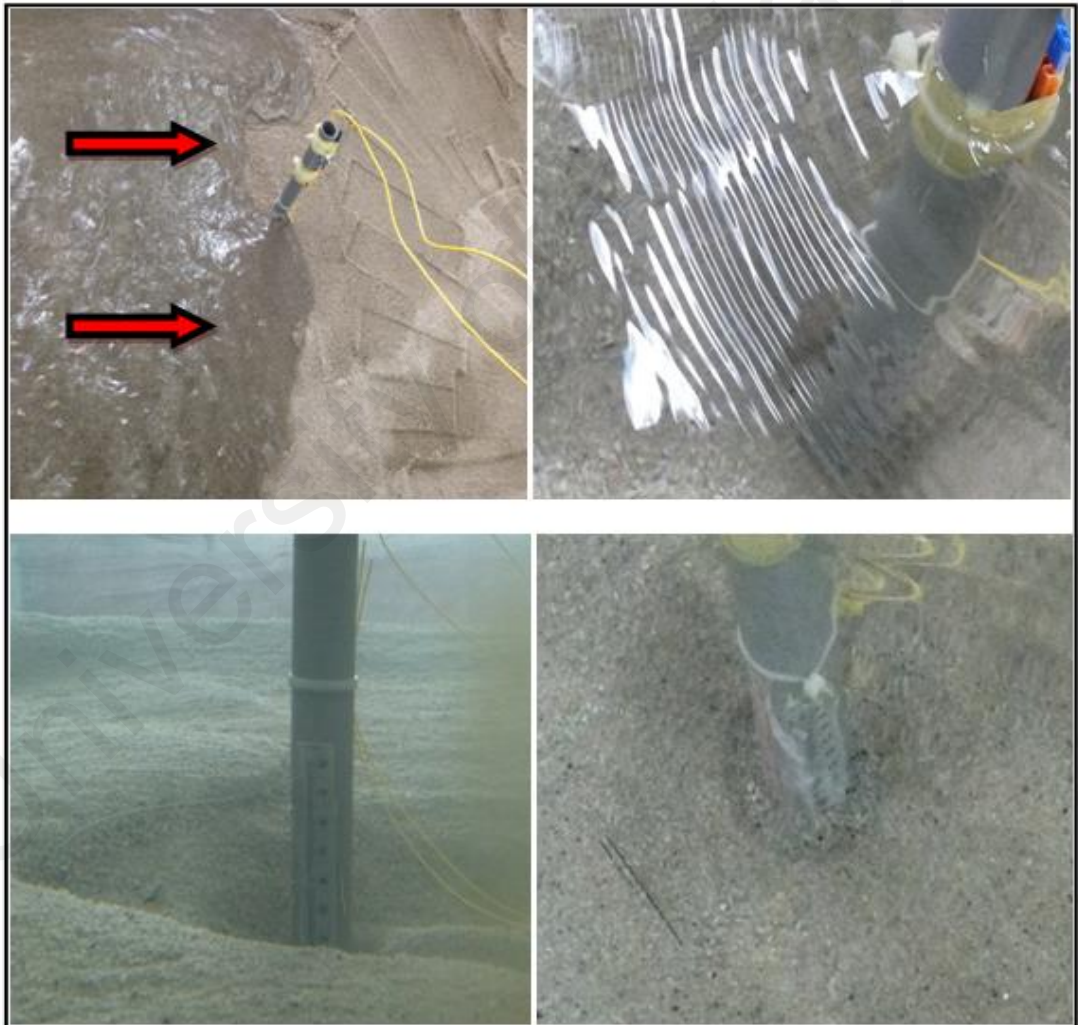


Figure 3.16: Images of the sensor probe during the experiment

CHAPTER 4: RESULTS AND DISCUSSION

4.1. Scouring Result

Theoretically, upon reaching a certain flow velocity in the channel, the sediment particles close to the pier (PVC pipe) begin to move and scour is initiated. The eroded particles will follow the flow pattern and are carried from the front of the pier towards the downstream. Upon an increase in flow velocity, more and more particles will get dislodged, forming a scour hole increasing in size and depth with respect to time. The depth of scour increases with time until it attains the equilibrium condition. When the equilibrium is reached, the transport out of scour hole should be about equal to the supply of the scour hole. It was reported in many literatures that the achievement of equilibrium is defined if the variation of the scour depth is equal or less than 5% of the pier diameter in a period of 24 hours (Melville & Chiew, 1999; Sheppard, Odeh, & Glasser, 2004).

Table 4.1 summarizes the experimental result of scour using a PVC pipe model. It shows that the scouring increases with time. This table shows the result of the experiment for no countermeasure. Countermeasures for local scour at bridge piers can be divided to two types which are armoring countermeasure and flow altering devices. Hence, in this research we are using none of the countermeasure. The scouring is frequently increases from time to time. The effect of scouring is focused on the maximum scouring that occur surround the pipe. Other than that, scouring also determined with the time development which is the major area of interest (Refer Figure 4.1). The experimental test was run with the uniform sediment size which is $d_{50} = 0.8$ mm. The height of water flow is 355 mm with the velocity of 0.34 m/s. The result shows that the scour activity is not yet achieved its equilibrium condition. Fig. 4.1 shows the scour depth, d_s/B , which was measure around the PVC pipe against time. The scour depth is observed to increase over time. The maximum d_s/B value of 1.35 is obtained at 900 min.

Table 4.1: Result for experiment of scour using PVC pipe model. d_s is a scour depth, B is pier width and d_s/B is a dimensionless scour depth

| Time, t | d_{50} | d_s | B | d_s/B |
|---------|----------|-------|------|---------|
| (min) | (mm) | (mm) | (mm) | |
| 0 | 0.8 | 0 | 20 | 0 |
| 5 | 0.8 | 6 | 20 | 0.3 |
| 10 | 0.8 | 10 | 20 | 0.5 |
| 15 | 0.8 | 12 | 20 | 0.6 |
| 20 | 0.8 | 12 | 20 | 0.6 |
| 25 | 0.8 | 14 | 20 | 0.7 |
| 30 | 0.8 | 14 | 20 | 0.7 |
| 40 | 0.8 | 15 | 20 | 0.75 |
| 50 | 0.8 | 15 | 20 | 0.75 |
| 60 | 0.8 | 16 | 20 | 0.8 |
| 70 | 0.8 | 16 | 20 | 0.8 |
| 80 | 0.8 | 17 | 20 | 0.85 |
| 90 | 0.8 | 17 | 20 | 0.85 |
| 100 | 0.8 | 17 | 20 | 0.85 |
| 260 | 0.8 | 18 | 20 | 0.9 |
| 420 | 0.8 | 19 | 20 | 0.95 |
| 580 | 0.8 | 20 | 20 | 1 |
| 740 | 0.8 | 23 | 20 | 1.15 |
| 900 | 0.8 | 27 | 20 | 1.35 |

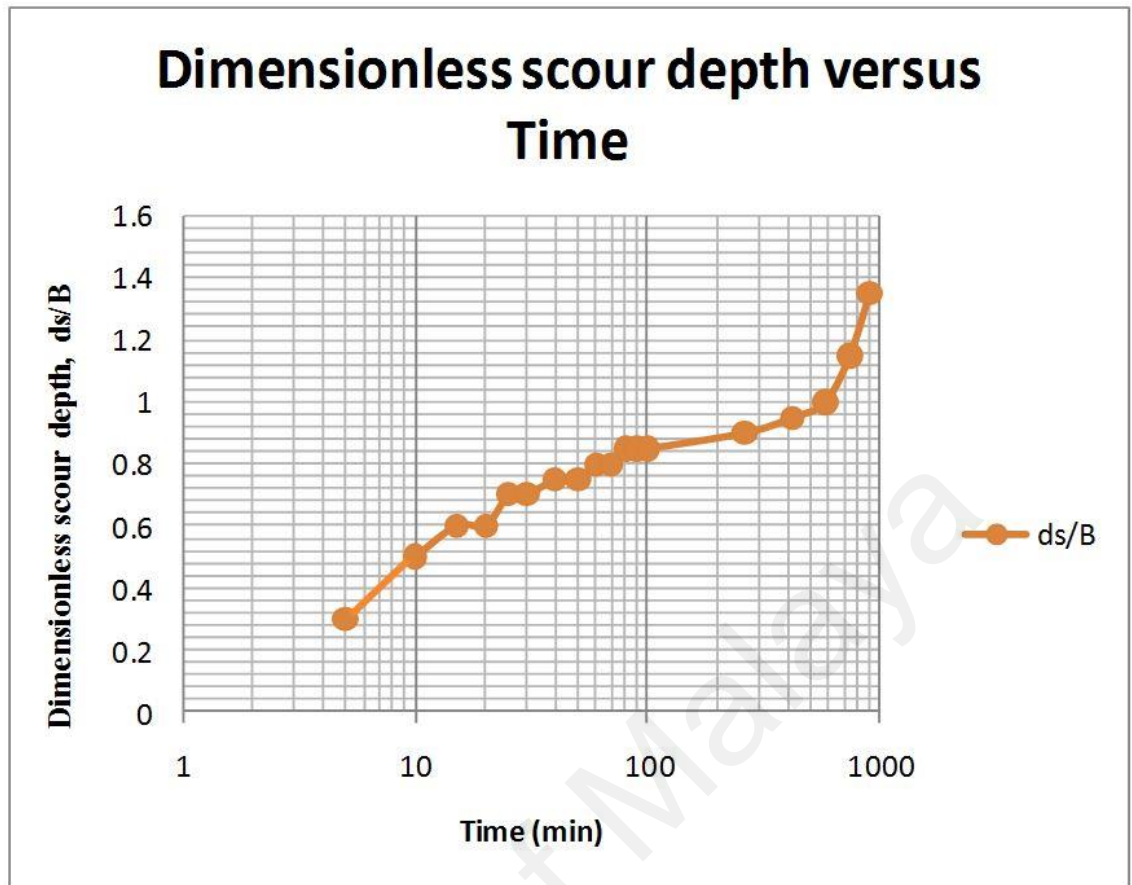


Figure 4.1: Scour depth, ds/B versus time scour occur at the PVC pipe

4.2. Bandpass Filtering Characteristic of SMS Structure

Fig. 4.2 shows the bandpass spectral response of the packaged SMS structure. In the experiment, ASE light centred at around 1550 nm is launched into the SMS structure and the transmitted spectrum is measured by an OSA. The packaging method of the SMS structure has been explained in the previous chapter to be robustly responsive to water flow and able to withstand sediment movement. It is observed that the spectrum has two significant dip at the wavelengths of 1526.68 nm and 1529.5 nm corresponding to the destructive multimode interference that occurs in the MMF section. Noted that the most prominent dip (λ_1) at 1526.68 nm is used to observe the spectral shift as the scour is developed at the PVC pipe. These dips are highly sensitive to strain and will be used to analyse the experimental data.

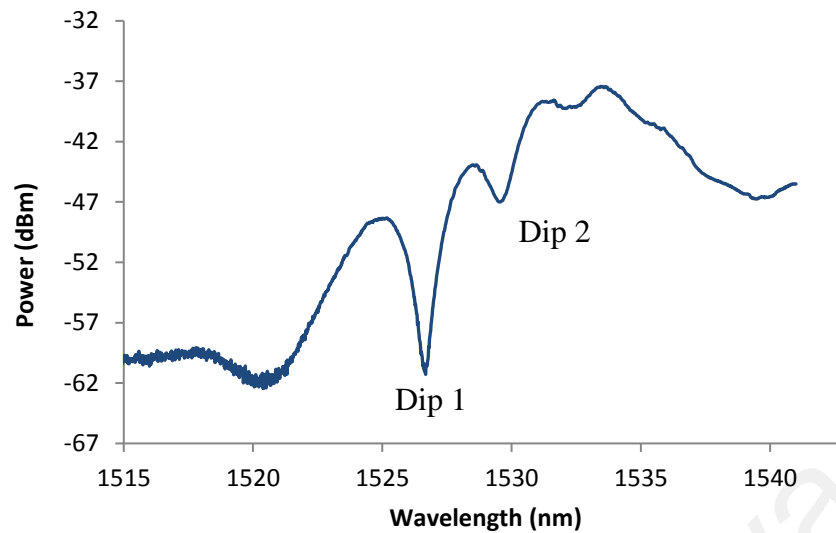


Figure 4.2: Bandpass filtering characteristic of the packaged SMS structure

4.3. Scouring Depth and Wavelength Change

The SMS sensor is attached to a concrete block, which is connected to the PVC pipe using water proof epoxy. The sensor and PVC pipe assembly was placed into a base of the hydraulic flume for monitoring of local scour activity. The detail sensor installation was described in the previous chapter. Fig. 4.3 shows the measured depth and scour depth curves at different time from 0 to 900 mins. The measured depth around pier was measured and recorded by depth meter with an accuracy of ± 1 mm while the scour depth values were calculated using Equation 3.1, based on the measured depth values. Measured depth will decrease by time and scour depth will increase with time increase. In phase 1, data were recorded every 10 min; from 0 mins to 100 mins. It can be observed that from 0 to 25 mins, there is a significant change of scour depth in an exponential manner, then the increase rate drops from 25 mins to 100 mins. In phase 2, which starts from 100 mins and lasts until 580 mins; the scour depth rate of change is smaller and linear with a value of 0.0063 mm/min as compared to that of phase 1. Data are recorded at a longer time interval of 160 mins in phase 2 since the scour depth changes at a slower rate. Overall,

the scour depth curve shows a similar pattern as clear-water scour where the bed material is not replaced at the scour hole after it is removed (Raudkivi & Ettema, 1983).

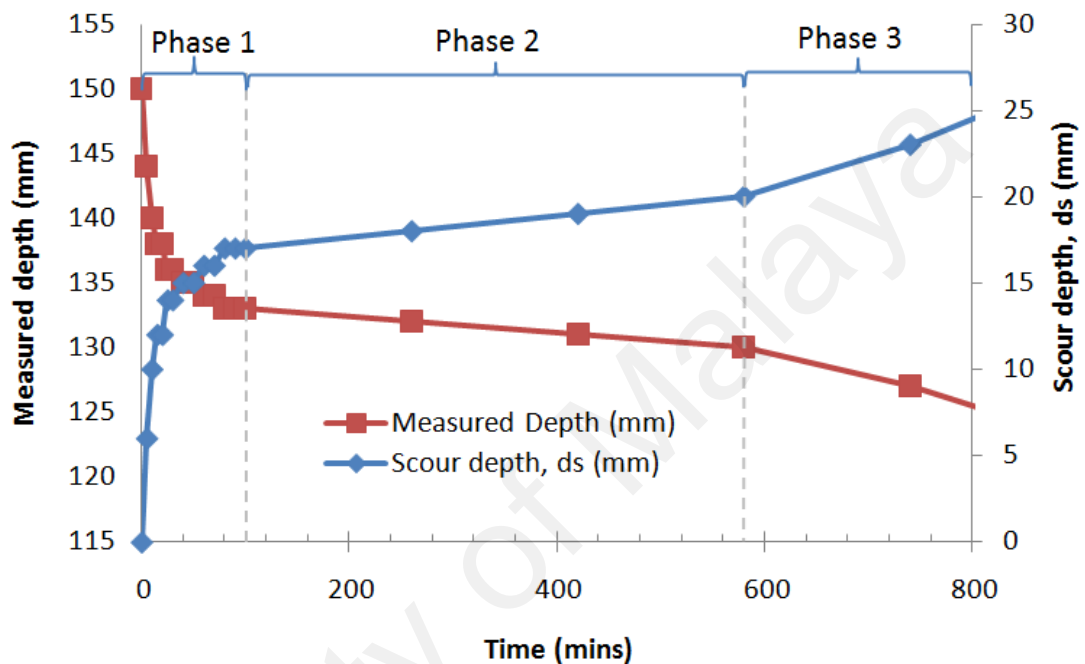


Figure 4.3: Measured depth and scour depth at different time interval

Phase 3 commences at 580 mins and ends at 900 mins. In this phase a regular water wave was generated at a constant speed of 0.03 m/s and wave amplitude of 140 mm. This was to further increase the scour depth rate of change with a value of 0.0219 mm/min. A maximum scour depth of 27 mm was obtained at 900 mins. Figure 4.4 and Figure 4.5 shows the photo images of the scour at the PVC pipe after 100 mins and 420 mins respectively. At 100 mins, a scour hole is observed and it is more obvious at 420 mins; with scour depth of 17 mm and 19 mm respectively. The sensor head is also noticeable.

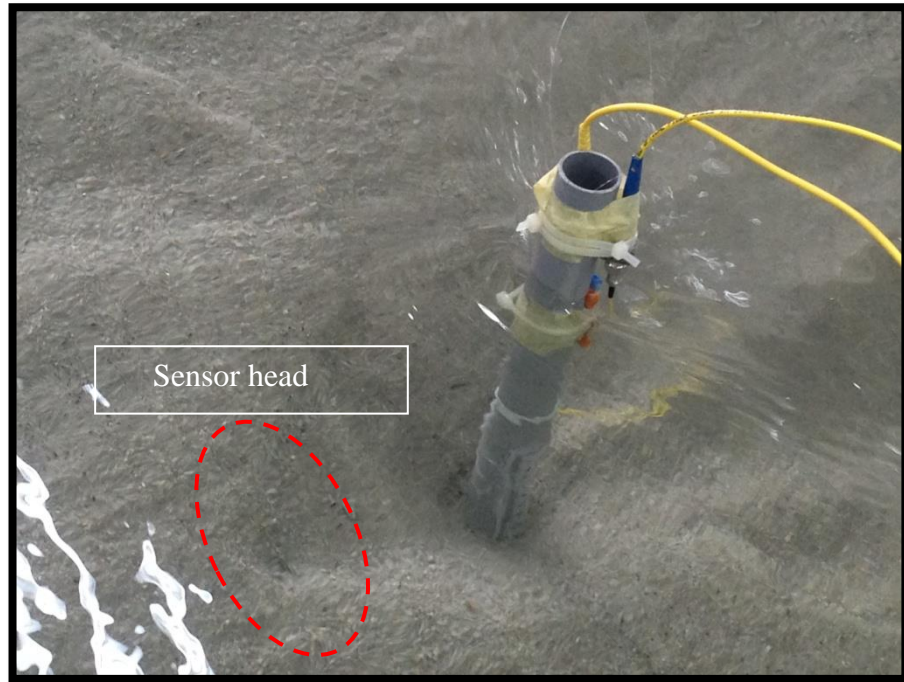


Figure 4.4: Photo images of PVC pipe scouring at different period of 100 mins

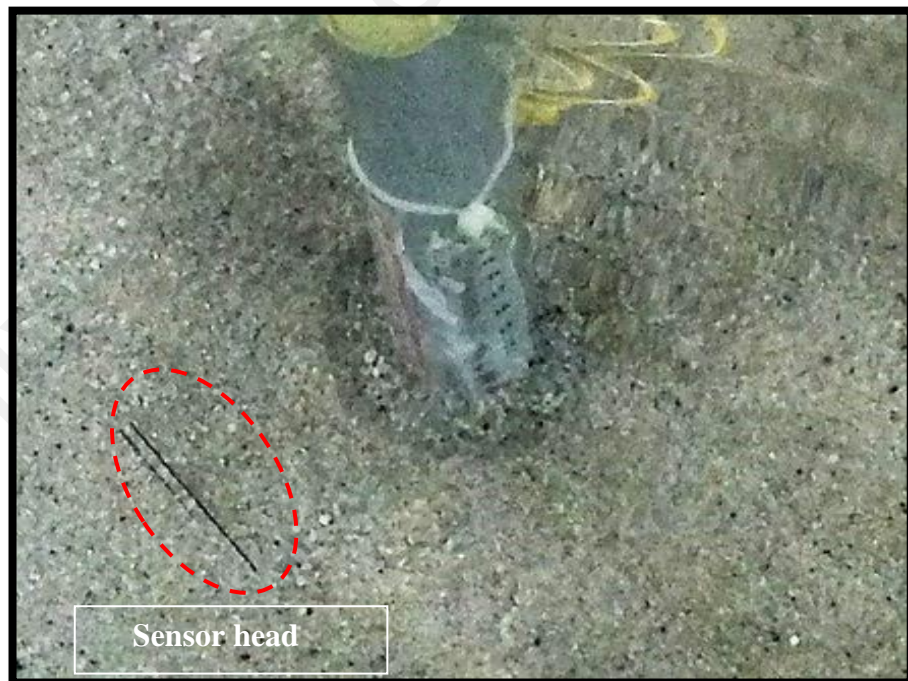


Figure 4.5: Photo images of PVC pipe scouring at different period of 420 mins

The sensor spectral wavelength shift is measured at a resolution of 0.05 nm. An increasing wavelength shift corresponding to the change of the scour depth is observed as shown in Figure. 4.6. The spectral analysis was focused at two dip wavelengths (λ_1 and λ_2) and their corresponding dip wavelengths values are plotted in Figs. 4.7 and 4.8. Dimensionless scour depth from Equation 3.2 is calculated and plotted together with the dip wavelengths as shown in Figs. 4.7 and 4.8. From Fig. 4.7, in phase 1, it is observed that the dip center wavelength 1 drops by 0.06nm and then it remains at a constant value with few fluctuations which is caused by noise coming from either temperature fluctuation or ASE noise. However, a significant change is seen in phase 2, wherein a wavelength shift of 0.12 nm is obtained first. This is followed by another shift of 0.06 nm. At this scour depth, a fraction of sediment has been removed at the top of the sensor as shown in Fig. 4.4; making it more sensitive. In phase 3, with the water wave, it is observed that the dip center wavelength 1 experiences a wavelength shift of 0.12 nm.

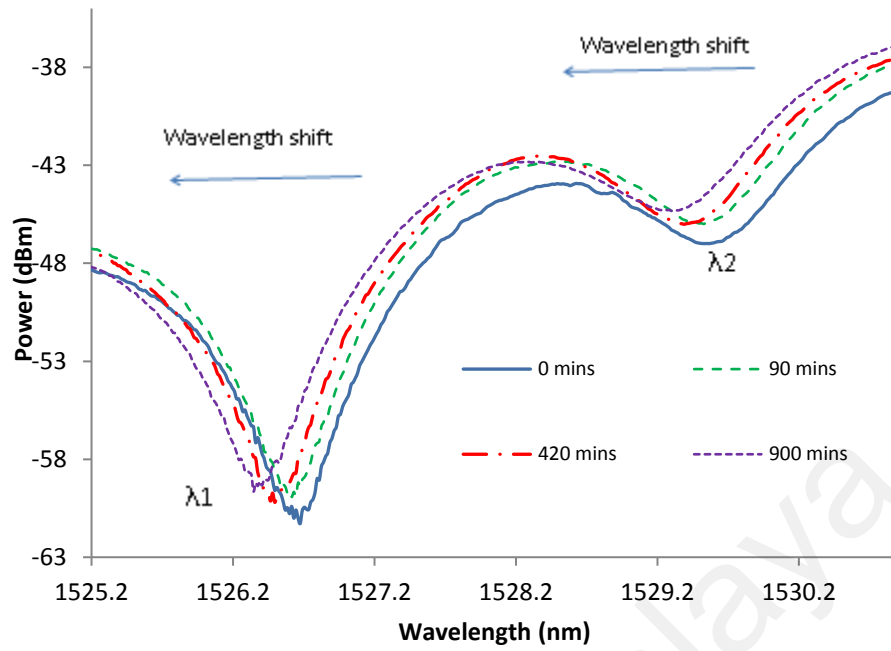


Figure 4.6: Sensor bandpass filter interferometer spectra at different time interval

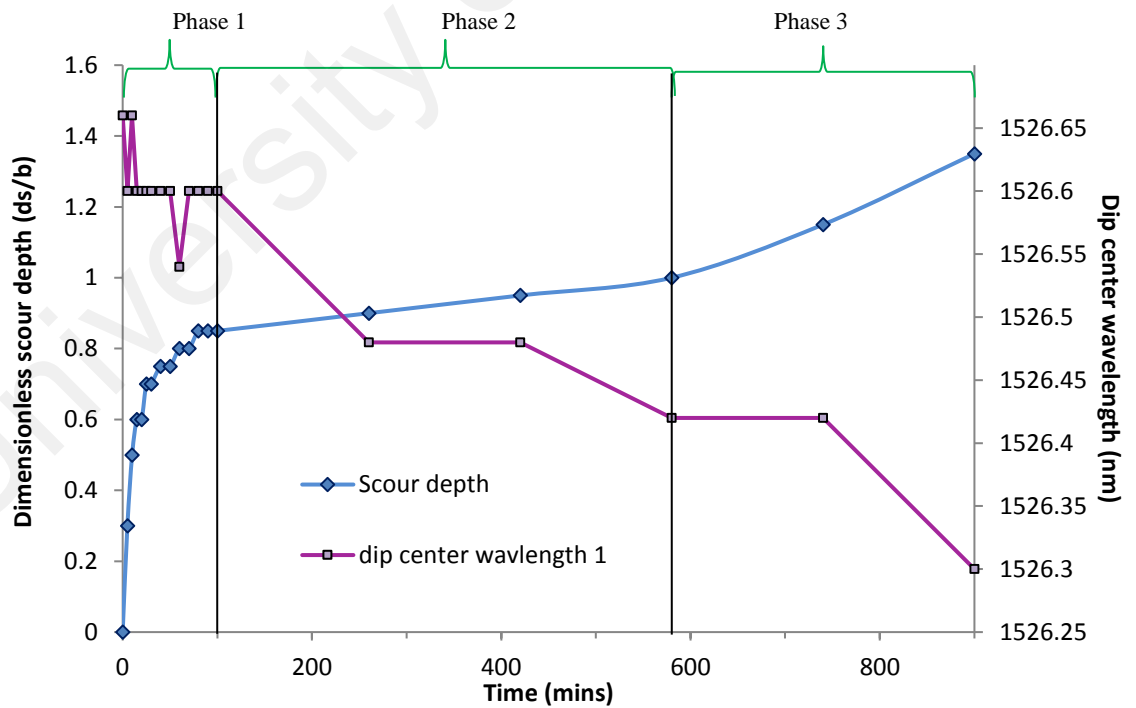


Figure 4.7: Dimensionless scour depth and dip center wavelength 1 curves for duration of 900 mins

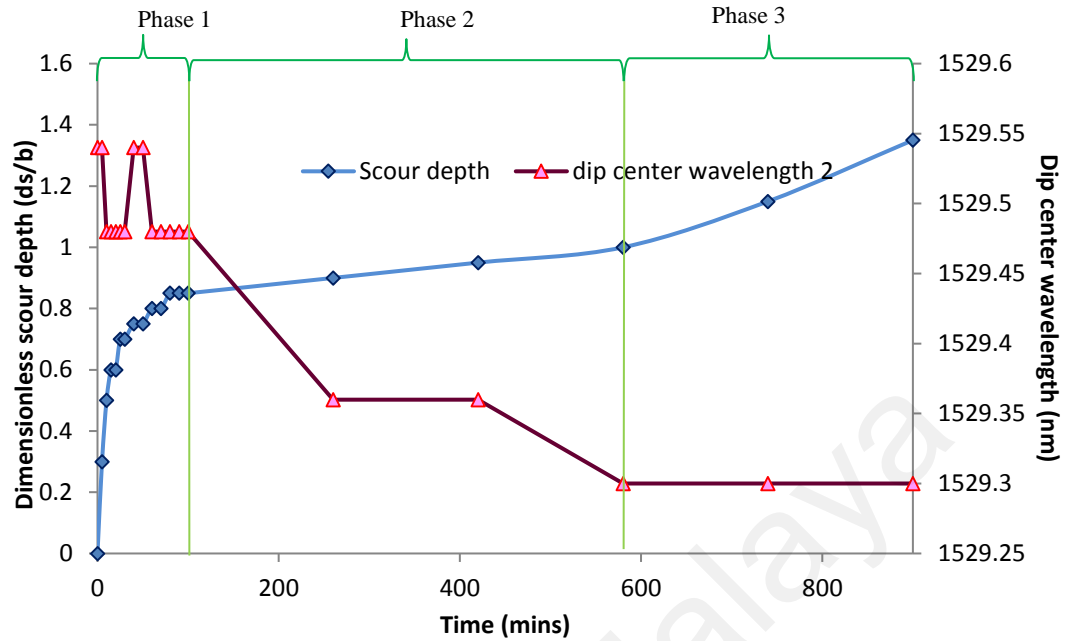


Figure 4.8: Dimensionless scour depth and dip center wavelength 2 curves for duration of 900 mins

In Fig. 4.8, it can be seen that dip centre of λ_2 experiences a similar wavelength shift. First, a wavelength shift of 0.06 nm is achieved in phase 1. In phase 2, a wavelength shift of 0.12 nm followed by another shift of 0.06 nm is recorded. However, there is no phase shift in phase 3. Overall, the largest wavelength shift of 0.12 nm is obtained for both dip centre wavelengths in phase 2. In this period, a larger fraction of sediment is removed at the top of the sensor head thus increasing its sensitivity. Another noticeable wavelength shift for dip centre wavelength occurs at the end of phase 3. It seems there is a noticeable change in scouring depth as well with a value of 1.35 from 1.15. Furthermore, it is observed that the scouring depth was still increasing after phase 3, therefore a longer duration of time is still needed to analyze the development of the local scour and the spectrum from the SMS sensor. Moreover, in the future, a better packaging and assembly method needs to be developed for this sensor before it can be use in a practical application.

CHAPTER 5: CONCLUSION AND FUTURE WORK RECOMMENDATION

5.1. Conclusion

We have developed a single-mode-multimode-single-mode (SMS) sensor system to detect PVC pipe scouring in conjunction with a new packaging method. A new packaging method for the sensor is developed to detect the extent of local scour using plastic monomer plate which is responsive to water flow. A set of experiments are performed using hydraulic flume for a duration of 900 mins with a maximum scour depth of 27 mm. Local scour formation shows a similar pattern to clear-water scour where the bed material is not replaced at the scour hole after it is removed. The SMS sensor is responsive to local scour via the change of spectral wavelength. Based on the findings of this research, the following conclusions could be drawn:

- 1) SMS sensor system has been successfully developed with a new packaging method that has a water resist characteristic.
- 2) The sensor was able to detect PVC pipe scouring.
- 3) Wavelength shifts of 0.12 nm and 0.06 nm are observed at the transitions between different phases in the development of local scour.

From the results and analysis, there is still room for improvement in the design and the installation method of the sensor either to improve its sensitivity and practical aspect. Overall, the results show promising potential for a real-time monitoring application such as in bridge scouring.

5.2. Recommendations for Further Investigation.

The results show that the SMS sensor has a potential to be applied in a real-time scour monitoring application surrounding the bridge piers. However, there are some caveats that must be addressed in future work. First, the sensitivity of the SMS sensor should be improved by optimizing the sensor structure, its packaging and assembly.

Second, new ways of installing the package must be identified, so the whole SMS technology is all well streamlined.

University of Malaya

REFERENCES

Akib, S., Fayyadh, M. M., & Othman, I. (2011). Structural behaviour of a skewed integral bridge affected by different parameters. *J. Road Bridge Eng*, 6(2), 107-114.

Akib, S., Jahangirzadeh, A., & Basser, H. (2014). Local scour around complex pier groups and combined piles at semi-integral bridge. *Journal of Hydrology and Hydromechanics*, 62(2), 108-116.

Akib, S., Liana Mamat, N., Basser, H., & Jahangirzadeh, A. (2014). Reducing Local Scouring at Bridge Piles Using Collars and Geobags. *The Scientific World Journal*, 2014.

Akib, S., Mashodi, N., Jahangirzadeh, A., & Shirazi, S. (2013). Semi-integral bridge scour countermeasure using gabion and crushed concrete mixed with Palm shell: a review. *Journal of Science and Technm {2B}*, 59, 68.

Akib, S., Mohammadhassani, M., & Jahangirzadeh, A. (2014). Application of ANFIS and LR in prediction of scour depth in bridges. *Computers & Fluids*, 91, 77-86.

Akib, S., Othman, F., Othman, I., Amini, A., & Marzuki, M. S. (2009). *Local scour at integral bridges with single and double row piles in a two-stage channel*. Paper presented at the H2009: 32nd Hydrology and Water Resources Symposium, Newcastle: Adapting to Change.

Amini, A., Melville, B. W., Ali, T. M., & Ghazali, A. H. (2011). Clear-water local scour around pile groups in shallow-water flow. *Journal of Hydraulic Engineering*.

Anderson, N. L., Ismael, A. M., & Thitimakorn, T. (2007). Ground-penetrating radar: a tool for monitoring bridge scour. *Environmental & Engineering Geoscience*, 13(1), 1-10.

Bin Lin, Y., Chang, K. C., Lai, J. S., & Wu, I. W. (2004). Applications of optical fiber sensor on local scour monitoring. In D. Rocha, P. M. Sarro & M. J. Vellekoop (Eds.), *Proceedings of the Ieee Sensors 2004, Vols 1-3* (pp. 832-835). New York: Ieee.

Bin Lin, Y., Lai, J. S., Chang, K. C., & Li, L. S. (2006). Flood scour monitoring system using fiber Bragg grating sensors. *Smart Materials & Structures*, 15(6), 1950-1959.

De Falco, F., & Mele, R. (2002). The monitoring of bridges for scour by sonar and sediment. *NDT & E International*, 35(2), 117-123.

Deng, L., & Cai, C. (2009). Bridge scour: Prediction, modeling, monitoring, and countermeasures—Review. *Practice periodical on structural design and construction*.

Ettema, R., Nakato, T., & Muste, M. V.-I. (2006). An illustrated guide for monitoring and protecting bridge waterways against scour: IIHR-Hydroscience & Engineering, University of Iowa.

Forde, M., McCann, D., Clark, M., Broughton, K., Fenning, P., & Brown, A. (1999). Radar measurement of bridge scour. *NDT & E International*, 32(8), 481-492.

Gao, R. X., Wang, Q., Zhao, F., Meng, B., & Qu, S. L. (2010). Optimal design and fabrication of SMS fiber temperature sensor for liquid. *Optics Communications*, 283(16), 3149-3152.

Hatta, A. M., Semenova, Y., Wu, Q., & Farrell, G. (2010). Strain sensor based on a pair of single-mode-multimode-single-mode fiber structures in a ratiometric power measurement scheme. *Applied Optics*, 49(3), 536-541.

Hunt, B. (2005). Scour monitoring programs for bridge health. *Transportation Research Record: Journal of the Transportation Research Board*(11s), 531-536.

King, N. S., & Mahamud, K. (2009). *Bridge Problems In Malaysia*. Paper presented at the Seminar in Bridge Maintenance and Rehabilitation. Kuala Lumpur.

Lagasse, P. F., & Richardson, E. V. (2001). ASCE compendium of stream stability and bridge scour papers. *Journal of Hydraulic Engineering*, 127(7), 531-533.

Lança, R., Fael, C., & Cardoso, A. (2010). Assessing equilibrium clear water scour around single cylindrical piers.

Lin, Y. B., Chen, J. C., Chang, K. C., Chern, J. C., & Lai, J. S. (2005). Real-time monitoring of local scour by using fiber Bragg grating sensors. *Smart Materials & Structures*, 14(4), 664-670.

Melville, B. W., & Coleman, S. E. (2000). *Bridge scour*: Water Resources Publication.

Melville, B. W., & Chiew, Y.-M. (1999). Time scale for local scour at bridge piers. *Journal of Hydraulic Engineering*, 125(1), 59-65.

Melville, B. W., Parola, A. C., & Coleman, S. E. (2008). Bridge-scour prevention and countermeasures. *Sedimentation engineering: processes, measurements, modeling, and practice, ASCE manuals and reports on engineering practice*(110), 543-577.

Moncada-M, A., Aguirre-Pe, J., Bolivar, J., & Flores, E. (2009). Scour protection of circular bridge piers with collars and slots. *Journal of Hydraulic Research*, 47(1), 119-126.

Raudkivi, A. J., & Ettema, R. (1983). Clear-water scour at cylindrical piers. *Journal of Hydraulic Engineering*, 109(3), 338-350.

Ruiz-Pérez, V., Basurto-Pensado, M., LiKamWa, P., Sánchez-Mondragón, J., & May-Arrijoja, D. (2011). *Fiber optic pressure sensor using multimode interference*. Paper presented at the Journal of Physics: Conference Series.

Sheppard, D. M., Odeh, M., & Glasser, T. (2004). Large scale clear-water local pier scour experiments. *Journal of Hydraulic Engineering*, 130(10), 957-963.

Simarro, G., Fael, C. M., & Cardoso, A. H. (2011). Estimating equilibrium scour depth at cylindrical piers in experimental studies. *Journal of Hydraulic Engineering*, 137(9), 1089-1093.

Wu, Q., Hatta, A., Wang, P., Semenova, Y., & Farrell, G. (2010). Use of a bent single SMS fiber structure for simultaneous measurement of displacement and temperature sensing.

Xiong, W., Cai, C. S., & Kong, X. (2012). Instrumentation design for bridge scour monitoring using fiber Bragg grating sensors. *Applied Optics*, 51(5), 547-557.

Yankielun, N., & Zabilansky, L. (1999). Laboratory investigation of time-domain reflectometry system for monitoring bridge scour. *Journal of Hydraulic Engineering*, 125(12), 1279-1284.

Yu, X., & Zabilansky, L. J. (2006). Time Domain Reflectometry for Automatic Bridge Scour Monitoring. *Site and Geomaterial Characterization*, 152.

Zhou, D.-P., Wei, L., Liu, W.-K., & Lit, J. W. (2009). Simultaneous strain and temperature measurement with fiber Bragg grating and multimode fibers using an intensity-based interrogation method. *Photonics Technology Letters, IEEE*, 21(7), 468-470.

Zhou, Z., Huang, M., Huang, L., Ou, J., & Chen, G. (2011). An optical fiber Bragg grating sensing system for scour monitoring. *Advances in Structural Engineering*, 14(1), 67-78.

University of Malaya

LIST OF PUBLICATIONS AND PAPERS PRESENTED

1. **N.M.Azmi**, N.H. Yusof, Z.Jusoh, H.A.Razak, S.W.Harun. Robust strain sensor based on multimode interference in single-mode–multimode–single- mode fiber structure. Optoelectronics and Advanced Materials – Rapid Communications vol. 12, iss. 5-6/2018.Published on 7th June 2018.
2. A.Z.Zulkifli ; S.E.F.Masnan ; **N.M.Azmi** ; S.M.Akib ; H.Arof ; S.W.Harun. A simple load sensor based on a bent single-mode-multimode-single-mode fiber structure. Sensors and Actuators. Published 1st May 2016.
3. S. E. F. Masnan ; A. Z. Zulkifli ; N. M. Azmi ; S. M. Akib ; H. A. Razak ; H. Arof ; S. W. Harun. Steel Beam Compressive Strain Sensor Using Single-mode Multi-mode Single-mode Fiber Structure. Photonic Journal, IEEE. Published on 3rd February 2016